A new view of an old suture zone: Evidence for sinistral transpression in the Cheyenne belt

W.A. Sullivan[1,†] and R.J. Beane[2]
[1]*Department of Geology, Colby College, 5803 Mayflower Hill, Waterville, Maine 04901, USA*
[2]*Department of Earth and Oceanographic Science, Bowdoin College, 6800 College Station, Brunswick, Maine 04011, USA*

ABSTRACT

The type locality of the Archean–Paleoproterozoic suture zone in the southern Rocky Mountains is marked by a series of subvertical shear zones collectively called the Cheyenne belt. The Cheyenne belt is a key structure for developing models for 1780–1740 Ma tectonism along the southern margin of the Archean Wyoming Province, which heralded a rapid period of continental amalgamation. This paper tests existing structural and plate-tectonic models for the Cheyenne belt with detailed geologic mapping, kinematic analyses, quartz crystallographic fabric analyses, and deformation mechanism analyses of the northern mylonite zone of the eastern Medicine Bow Mountains. Mylonites of this zone record a complex deformation history, but the main deformation phase was sinistral/northwest-side-up oblique transpression. Evidence for southeast-side-up, dip-slip motion that characterizes many other areas of the belt is confined to ultramylonites immediately adjacent to the terrane boundary. Hence, fabrics related to sinistral transpression were likely overprinted by southeast-side-up motion. Sinistral strike-slip motion is recorded in at least two other localities in the Cheyenne belt. Because synmetamorphic fabrics on both sides of the suture zone record sinistral strike-slip and northwest-side-up motion, this was probably the dominant deformation style in the field area and may have been the dominant deformation style throughout the Cheyenne belt. Based on these data and regional constraints, we interpret the Cheyenne belt as a subvertical transpressional stretching fault system that simultaneously accommodated sinistral strike-slip motion, penetrative horizontal shortening, and dip-slip motion related to differential crustal thickening between the relatively cold Wyoming Province and younger, hotter rocks to the south.

[†]E-mail: wasulliv@colby.edu

INTRODUCTION

The Medicine Bow Mountains and Sierra Madre in southeastern Wyoming present one of the best records of Paleoproterozoic plate-tectonic processes in North America (Fig. 1) (Whitmeyer and Karlstrom, 2007). Rocks in this area record: (1) rifting and formation of a passive margin along the southern margin of the Archean Wyoming Province beginning around 2010 Ma, followed by (2) reactivation of the passive margin and accretion of the Green Mountain terrane of the Colorado Province during the 1780–1740 Ma Medicine Bow orogeny (e.g., Hills and Houston, 1979; Karlstrom and Houston, 1984; Duebendorfer and Houston, 1987; Chamberlain, 1998; Jones et al., 2010). The tectonic reactivation of the southern margin of the Wyoming Province was the start of a rapid period of continental amalgamation as an ~1000-km-wide belt of relatively juvenile crust collectively known as the Colorado Province was added to the Archean cratons of North America over a 140–170 m.y. period (Hoffman, 1988; Bowring and Karlstrom, 1990; Bickford and Hill, 2007; Whitmeyer and Karlstrom, 2007).

The fundamental boundary between the Archean Wyoming Province and the ca. 1800–1650 Ma rocks of the Colorado Province is called the Cheyenne belt (Fig. 1) (Houston et al., 1968; Hills and Houston, 1979; Karlstrom and Houston, 1984; Duebendorfer and Houston, 1987). The type locality of the Cheyenne belt is located in the Medicine Bow Mountains (Fig. 1), where it is marked by a set of northeast-striking, subvertical shear zones. The movement history of these shear zones is one of the key lines of evidence used to develop structural and plate-tectonic models for the Medicine Bow orogeny and the amalgamation of the Colorado and Wyoming Provinces (Hills and Houston, 1979; Duebendorfer and Houston, 1987; Chamberlain, 1998). Historically, these shear zones have been interpreted as part of a strike-slip fault system (Warner, 1978); a high-angle reverse fault system representing a paleo–subduction zone (Hills and Houston, 1979); a gently dipping, crustal-scale thrust fault system rotated into its present subvertical orientation during late-stage, orogen-scale folding (Karlstrom and Houston, 1984; Duebendorfer and Houston, 1986, 1987; Duebendorfer, 1988); and a crustal-scale stretching fault that accommodated differential crustal thickening during the Medicine Bow orogeny (Sullivan et al., 2011). The thrust fault model is the most widely accepted, and it has led to plate-tectonic models that invoke near-orthogonal collision during the Medicine Bow orogeny (Hills and Houston, 1979; Duebendorfer and Houston, 1987; Chamberlain, 1998; Jones et al., 2010). The thrust fault model is based on five lines of evidence: (1) Lineations in the Cheyenne belt shear zones are typically steeply plunging; (2) kinematic analyses of L-S tectonites from the frontal shear zone indicate southeast-side-up motion; (3) foliations and bedding are generally subparallel with the tectonic contacts; (4) metamorphic grade increases abruptly across the shear zones toward the southeast; and (5) large horizontal displacements are needed to juxtapose the widely different rock units exposed across the Cheyenne belt (Hills and Houston, 1979; Karlstrom and Houston, 1984; Duebendorfer and Houston, 1986, 1987; Duebendorfer, 1988).

All five lines of evidence used to support the thrust fault model also can be explained by transpressional deformation with strike-slip motion and penetrative horizontal shortening coupled with vertical elongation. First, detailed examinations of transpressional shear zones and strain modeling indicate that the subvertical foliations, apparent flattening strains, and subvertical lineations found throughout the Cheyenne belt are compatible with tectonic transpression (e.g., Fossen and Tikoff, 1993; Greene and Schweickert, 1995; Dutton, 1997; Dewey et al., 1998; Jiang and Williams, 1998; Czeck and Hudleston, 2003; Jones et al., 2004; Kuiper et al., 2011). Second, transpression zones that localize horizontal shortening coupled with vertical elongation require localized dip-slip stretching

GSA Bulletin; July/August 2013; v. 125; no. 7/8; p. 1319–1337; doi: 10.1130/B30679.1; 14 figures.

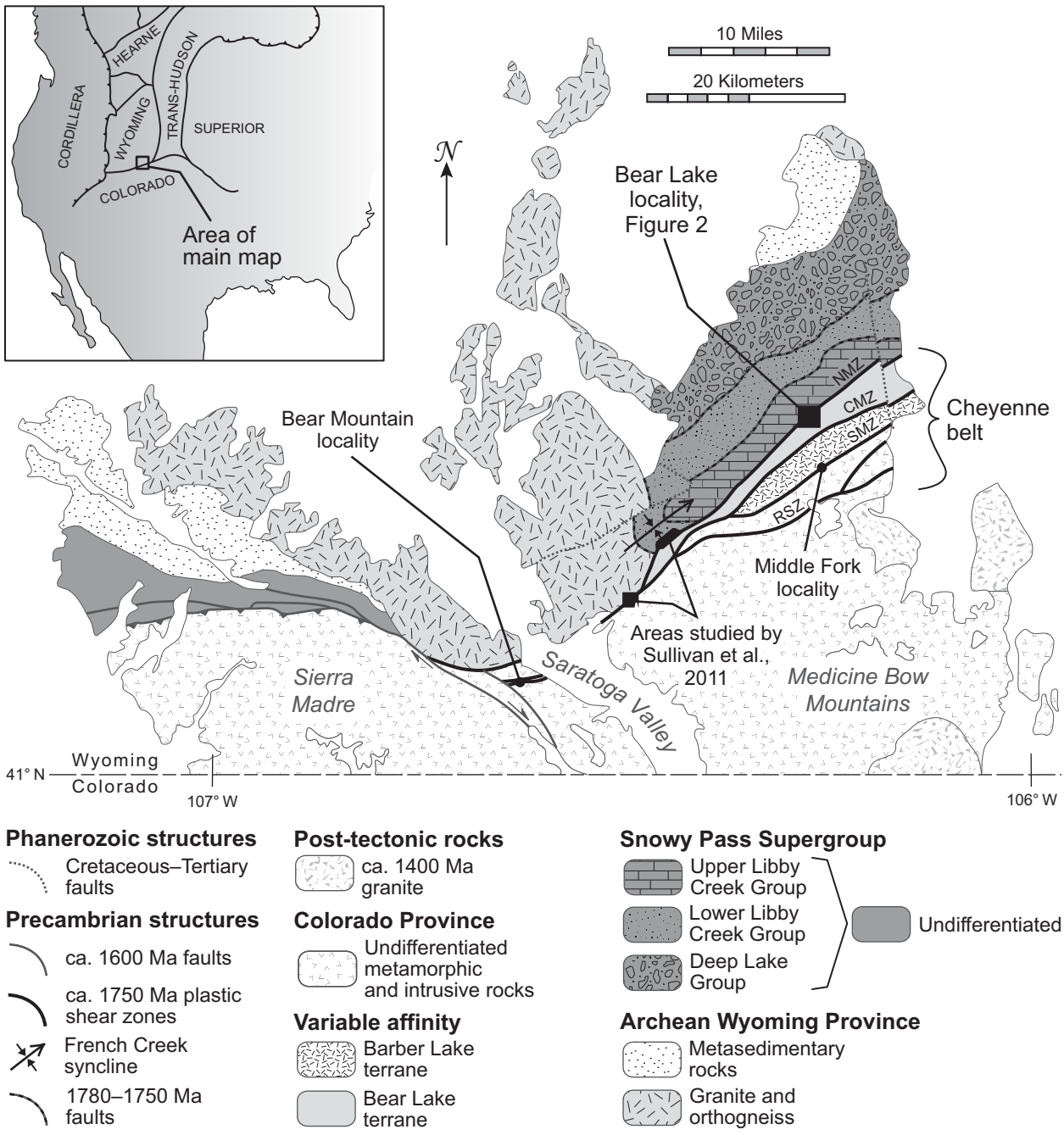

Figure 1. Map of Precambrian rocks exposed in the Medicine Bow Mountains and Sierra Madre in southeastern Wyoming showing the locations of major fault zones of the Cheyenne belt: NMZ—northern mylonite zone, CMZ—central mylonite zone, SMZ—southern mylonite zone, and RSZ—Rambler shear zone. The area of Figure 2 and other areas discussed in the text are also shown. Inset map shows the major Precambrian basement provinces of the western United States and western Canada. Data are compiled from Houston et al. (1968), Duebendorfer (1990), Houston and Karlstrom (1992), Houston and Graff (1995), and Resor and Snoke (2005). Figure is modified from Sullivan et al. (2011).

faults (Means, 1989) to maintain strain compatibility at their margins (Dewey et al., 1998). This localization of stretching faults could explain the southeast-side-up motion recorded in the frontal shear zone of the Cheyenne belt (Sullivan et al., 2011). Third, long-lived transpression also should create foliations parallel with tectonic boundaries and rotate bedding parallel with these boundaries. Fourth, localized horizontal shortening coupled with vertical elongation would have driven more rapid exhumation of high-grade rocks in the Cheyenne belt and, therefore, can explain the observed southward increase in metamorphic grade. Finally, strike-slip motion can easily juxtapose different rock units. Therefore, it is plausible that the main phase of deformation in the Cheyenne belt shear zones occurred while they were subvertical, and

that this deformation was transpressional. If this transpression hypothesis is correct, a new structural model for the Medicine Bow orogenic belt is needed, and plate-tectonic models for terrane amalgamation along the southern margin of the Wyoming Province should be revised to account for strike-slip motion in the type locality of the Cheyenne belt.

Both the rotated thrust fault and transpression models for the Cheyenne belt provide a number of testable predictions (Table 1). These tests fall into two categories: (1) detailed, across-strike kinematic analyses of the subvertical high-strain zones in the Cheyenne belt, which may reveal previously undocumented strain partitioning and localized strike-slip motion; and (2) combined quantitative thermobarometry, thermochronology, and geochronology, which may help to constrain pressure-temperature-time (*P-T-t*) paths across the Medicine Bow orogeny. We focus on the first of these two categories as a gateway to the more costly and involved thermobarometry, thermochronology, and geochronology. Hence, this contribution integrates detailed geologic mapping, kinematic analyses of S and L-S tectonites, quartz crystallographic fabric analyses, and deformation mechanism analyses of the frontal deformation zone of the Cheyenne belt adjacent to Bear Lake in the eastern Medicine Bow Mountains (Figs. 1 and 2). This study area is hereafter referred to as the Bear Lake locality. Data from the Bear Lake locality along with reconnaissance-level data from two other sites indicate that sinistral strike-slip motion was accommodated across the Cheyenne belt. These new data are integrated with regional constraints to produce a new conceptual model for the Medicine Bow orogeny in the type locality of the Cheyenne belt.

REGIONAL GEOLOGY

Shear Zones of the Cheyenne Belt

In the Medicine Bow Mountains, the Cheyenne belt appears as an eastward-branching set of northeast-striking, subvertical deformation zones that separate distinct lithotectonic terranes (Fig. 1) (Houston et al., 1968; Hills and Houston, 1979; Karlstrom and Houston, 1984; Duebendorfer and Houston, 1986, 1987; Duebendorfer, 1990; Houston and Karlstrom, 1992). There are four deformation zones in the central and eastern Medicine Bow Mountains (Houston et al., 1968; Duebendorfer, 1990; Karlstrom and Houston, 1992). From north to south, these zones are named the northern mylonite zone, central mylonite zone, southern mylonite zone, and Rambler shear zone (Fig. 1) (Duebendorfer and Houston, 1987; Houston, 1993). In most areas, terrane juxtaposition was largely accomplished by plastic deformation under amphibolite-facies conditions (Duebendorfer, 1986; Duebendorfer and Houston, 1986, 1987). Available direct dates of this amphibolite-facies deformation all are ca. 1750 Ma (Strickland, 2004; Duebendorfer et al., 2006).

Reconnaissance-level microstructural and quartz *c*-axis fabric analyses from the length of the northern mylonite zone indicate southeast-side-up, dip-slip or oblique-slip motion (Duebendorfer, 1986; Duebendorfer and Houston, 1986, 1987). Two detailed across-strike studies of the northern mylonite zone in the western Medicine Bow Mountains corroborate these results and also show that significant strain partitioning occurred in at least part of the Cheyenne belt (Sullivan et al., 2011). In the far western Medicine Bow Mountains, where the belt narrows to a single deformation zone (Fig. 1), lower-amphibolite-facies deformation fabrics record significant coaxial horizontal shortening and relatively minor southeast-side-up motion (Sullivan et al., 2011). To the east of this area, lower-amphibolite-facies deformation fabrics in the northern mylonite zone record significant southeast-side-up motion and partitioned coaxial horizontal shortening (Sullivan et al., 2011).

Throughout most of the Sierra Madre, the ca. 1750 Ma, amphibolite-facies shear zones of the Cheyenne belt were truncated by 1590–1620 Ma brittle faults that now form the terrane boundaries in this area (Fig. 1) (Houston and Graff, 1995; Duebendorfer et al., 2006). There is no evidence that ca. 1600 Ma deformation significantly modified the terrane boundaries in or near the Bear Lake locality (Duebendorfer, 1986).

Terranes Juxtaposed across the Cheyenne Belt

Wyoming Province

The oldest known rocks north of the Cheyenne belt are Neoarchean orthogneiss and foliated granite exposed along the western flank of the Medicine Bow Mountains (Fig. 1) (Houston et al., 1968; Hills et al., 1968; Premo and Van Schmus, 1989). Within 1 km of the Cheyenne belt, gneissic banding and foliations in the Archean rocks are rotated parallel with the northeast-striking, subvertical Paleoproterozoic deformation fabrics (Houston et al., 1968; Sullivan et al., 2011). Elsewhere in the Medicine Bow Mountains, Archean deformation fabrics are north-northwest to west striking with variable dips that reflect polyphase folding (Houston et al., 1968).

Archean rocks are overlain by the Paleoproterozoic Snowy Pass Supergroup (Fig. 1) (Houston et al., 1968; Karlstrom et al., 1983;

TABLE 1. PREDICTIONS MADE BY THE THRUST FAULT AND TRANSPRESSIONAL STRETCHING FAULT MODELS FOR THE CHEYENNE BELT

	Thrust fault model	Transpressional stretching fault model (this paper)
Kinematics		
Strike-slip motion	Not compatible outside lateral ramps	Expected
Southeast-side-up, dip-slip motion	Expected everywhere	Expected at northern edge of Cheyenne belt
Northwest-side-up, dip-slip motion	Not compatible	Possible in interior of Cheyenne belt or as early phase of deformation
Coaxial shortening	Possible everywhere	Possible everywhere
Metamorphic conditions		
North of Cheyenne belt	Highest pressure (*P*) rocks	Lowest *P* and *T* rocks
In the Cheyenne belt	High-*P* and high-temperature (*T*) rocks; syndeformational decompression possible	Highest *P* and *T* rocks; syndeformational decompression or compression possible
South of Cheyenne belt	Lowest *P* and *T* rocks; southward decrease in *P* and *T*	High- or low-*P* and -*T* rocks possible; high *P* and *T* probable
Geochronology		
P-T-t paths	Hanging-wall peak *P* and *T* at start of thrusting; footwall peak *P* at end of thrusting, peak *T* after thrusting	Peak *P* and *T* coeval across orogen

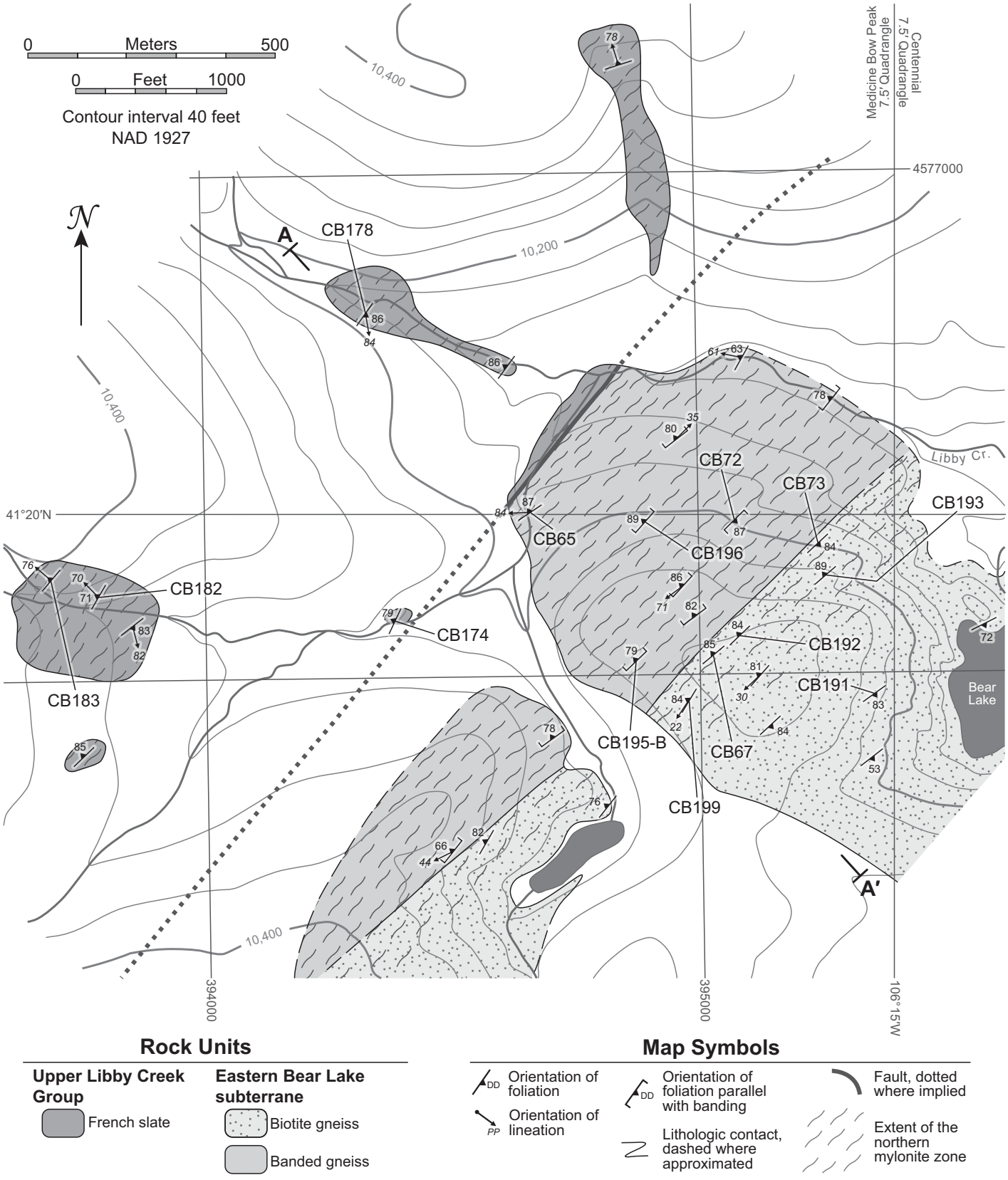

Figure 2. Geologic map of the Bear Lake locality showing the locations of samples and exposures discussed in the text or depicted in the figures. The sinusoidal pattern represents the extent of the northern mylonite zone, and its spacing intensity represents the relative deformation intensity observed in outcrop. Areas in white represent thick Quaternary alluvium.

Houston and Karlstrom, 1992). From bottom to top, the Snowy Pass Supergroup is composed of: (1) the ~3.6-km-thick Deep Lake Group, which primarily consists of polymictic metaconglomerate and quartzite; (2) the ~4.4-km-thick lower part of the Libby Creek Group, which primarily consists of quartzite; and (3) the ~3-km-thick upper part of the Libby Creek Group, which primarily contains metamorphosed dolostone and an uppermost ~1–1.5-km-thick black phyllite and slate member formally named the French Slate (Houston et al., 1968; Karlstrom et al., 1983; Houston and Karlstrom, 1992). The Deep Lake and lower Libby Creek Groups are intruded by numerous 2100–2000 Ma tholeiitic dikes and plugs, and they record rifting along the southern margin of the Wyoming Province (Hills and Houston, 1979; Karlstrom et al., 1983; Karlstrom and Houston, 1984). The upper Libby Creek Group is interpreted as a passive-margin sequence (Hills and Houston, 1979; Karlstrom et al., 1983; Karlstrom and Houston, 1984).

The Deep Lake Group and the lower and upper Libby Creek Group are all bounded by bedding-parallel faults widely interpreted as thrust faults (Fig. 1) (Houston et al., 1968; Karlstrom and Houston, 1984; Houston and Karlstrom, 1992). Bedding and faults in the Snowy Pass Supergroup are northeast striking and steeply dipping, except where they are deformed by the multi-kilometer-scale, steeply plunging French Creek syncline (Fig. 1) (Houston et al., 1968; Houston and Karlstrom, 1992). The syncline and the faults are truncated by the northern mylonite zone (Fig. 1) (Houston et al., 1968; Karlstrom and Houston, 1984; Houston and Karlstrom, 1992). Horses of lower Libby Creek Group quartzite are entrained in the northern mylonite zone east of the French Creek syncline. These horses must have been cut off from the French Creek syncline, and they exhibit ~8 km of sinistral separation (Houston and Karlstrom, 1992).

The French Slate contains a well-developed, northeast-striking, subvertical foliation that is parallel with bedding and sparse small isoclinal folds (Houston et al., 1968; Karlstrom and Houston, 1984). This deformation fabric is defined by prograde metamorphic minerals and is widely interpreted as coeval with the Cheyenne belt (Karlstrom and Houston, 1984; Duebendorfer, 1986; Duebendorfer and Houston, 1987; this study). Quartzites and metaconglomerates of the lower Libby Creek and Deep Lake Groups exhibit little or no internal deformation, whereas pelitic rocks of these units are strongly foliated and variably folded (Houston et al., 1968; Karlstrom and Houston, 1984).

Phyllite and slate of the French Slate have normal marine-shale bulk compositions and contain the prograde mineral assemblage chlorite + white mica + quartz + detrital K-feldspar (Karlstrom et al., 1983). Greenstones of the upper Libby Creek Group contain the prograde mineral assemblage actinolite + chlorite + epidote (Karlstrom et al., 1983). These mineral assemblages indicate peak metamorphic temperatures of ~400 °C or less (Spear and Cheney, 1989). Metamorphic grade in the French Slate systematically increases within 1 km of the Cheyenne belt, and the prograde assemblages staurolite + garnet + biotite and, in one sample, andalusite + kyanite + garnet + biotite are found within 50–100 m of the northern mylonite zone, ~1.5 km northeast of the Bear Lake locality (Duebendorfer, 1988). These mineral assemblages record metamorphic temperatures of 500 °C or more (Duebendorfer, 1988; Spear and Cheney, 1989).

Duebendorfer's (1988) description indicates that both Al_2SiO_5 polymorphs in the French Slate either predate or developed at the same time as the tectonic fabric related to the northern mylonite zone. A thrust fault model for the Cheyenne belt implies a relatively rapid pressure increase in the footwall during thrust motion followed by nearly isobaric heating as the thermal gradient between the hanging wall and footwall relaxed. A transpression model also implies nearly isobaric heating of rocks on the north side of the zone, but the *P-T-t* path is more analogous to contact metamorphism adjacent to a pluton. In either case, the French Slate should have passed from the kyanite stability field into the andalusite field during prograde metamorphism. Such a *P-T-t* path limits peak pressures on the northeast side (presumptive footwall) of the Cheyenne belt to the pressure of the Al_2SiO_5 triple point, or ~390 MPa (Hemmingway et al., 1991).

Terranes within the Cheyenne Belt

Two distinct lithotectonic terranes, bounded by shear zones of the Cheyenne belt, are exposed southeast of the Snowy Pass Supergroup in the central and eastern Medicine Bow Mountains. Following the terminology of Sullivan et al. (2011), these are referred to here as the Bear Lake terrane and Barber Lake terrane (Fig. 1). Note, we use the term terrane in the nongenetic, descriptive sense of Irwin (1972).

The Bear Lake terrane is juxtaposed with the French Slate across the northern mylonite zone (Fig. 1). The eastern subterrane of the Bear Lake terrane consists of polydeformed quartzofeldspathic orthogneiss, whereas the western subterrane consists of a bimodal sequence of tholeiitic orthoamphibolite and foliated granite (Duebendorfer, 1986; Duebendorfer and Houston, 1986, 1987). Rocks of the eastern subterrane yield Archean Nd model ages, and they are probably a slice of Archean Wyoming Province basement (Ball and Farmer, 1991). The age of the western subterrane is unknown. The eastern subterrane contains numerous upright to steeply dipping, gently plunging to subhorizontal, outcrop-scale, symmetrical folds that deform compositional layering in the gneiss (Duebendorfer and Houston, 1987). These folds tighten approaching the northern mylonite zone and become axial planar with the mylonitic foliation as gneissic banding is progressively transposed into parallelism with the shear zone (Duebendorfer and Houston, 1987; this study). Duebendorfer and Houston (1986, 1987) interpreted these folds as coeval with the Cheyenne belt deformation based on their orientations and their progressive intensification closer to the terrane-bounding shear zones.

The Barber Lake terrane is juxtaposed with the Bear Lake terrane across the central mylonite zone. It primarily consists of migmatitic paragneiss that hosts numerous meter- to kilometer-scale garnet-bearing biotite granite and leucogranite bodies (Duebendorfer and Houston, 1987). The paragneiss contains the prograde assemblage sillimanite + K-feldspar + melt, which indicates peak metamorphic temperatures of 650 °C or more (Duebendorfer and Houston, 1987; Spear and Cheney, 1989). Synmetamorphic titanite from these rocks yielded a U-Pb age of 1748 ± 10 Ma (Strickland, 2004). These rocks also yield 2000–2400 Ma Nd model ages and Archean detrital zircon, and their protolith must have formed near an Archean craton (Ball and Farmer, 1991; Jones, 2011). Synmetamorphic folds in this terrane are upright to steeply inclined, subhorizontal to reclined, and they are associated with a variably developed northeast-striking and steeply southeast-dipping foliation (Duebendorfer and Houston, 1987). These folds and foliations progressively tighten and intensify approaching the Cheyenne belt shear zones, where they are completely transposed into parallelism with the mylonitic foliations (Duebendorfer and Houston, 1987).

Rocks South of the Cheyenne Belt

A wide variety of igneous intrusive, metavolcanic, and metasedimentary rocks are exposed south of the Cheyenne belt in the Sierra Madre and Medicine Bow Mountains (Houston et al., 1968; Houston et al., 1989; Houston and Graff, 1995; Jones et al., 2010). These rocks are generally considered part of the Green Mountain arc (Condie and Shadel, 1984; Reed et al., 1987; Tyson et al., 2002). Because igneous rocks in this terrane record both arc magmatism and postarc extension (Jones et al., 2010, 2011), we refer to it as the Green Mountain terrane to avoid the genetic connotation of the term "arc." Arc-related igneous

rocks in the Green Mountain terrane include ca. 1774–1782 Ma layered mafic complexes, gabbro, diorite, tonalite, granite, and rhyolite porphyry (Premo and Van Schmus, 1989; Premo and Loucks, 2000; Jones et al., 2010, 2011). In the southeastern Sierra Madre, a voluminous ca. 1759–1769 Ma bimodal gabbro-granite suite intrudes the arc-related rocks, and probably records crustal extension after the end of arc magmatism (Jones et al., 2010). Rocks in the southeastern Sierra Madre experienced amphibolite-facies metamorphism and north-south–directed shortening at ca. 1750 Ma (Jones et al., 2010). To date, no detailed structural or geochronologic analyses have been conducted south of the Cheyenne belt in the Medicine Bow Mountains. However, the published 1:63,360 scale mapping and our reconnaissance-level observations show that lithologic contacts and foliations throughout the southern Medicine Bow Mountains are generally east to northeast striking and steeply dipping to subvertical over 30 km across orogenic strike south of the Cheyenne belt (Houston et al., 1968). Fabrics in deformed mafic rocks throughout this region are defined by amphibolite-facies mineral assemblages (Houston et al., 1968; Houston et al., 1989).

BEAR LAKE LOCALITY ROCK UNITS

French Slate

The French Slate lies entirely within the mapped extent of the northern mylonite zone (Fig. 2). Here it contains the prograde assemblage biotite + muscovite + quartz + plagioclase + garnet ± chlorite. Throughout the field area, this unit contains a strong, northeast-striking, steeply north-dipping to subvertical foliation defined by aligned biotite and muscovite and a moderate to strong downdip mineral lineation defined by biotite porphyroblasts and pressure-shadow overgrowths on porphyroblasts (Figs. 2 and 3A). Duebendorfer (1988) calculated metamorphic temperatures of 433 ± 18 °C and 449 ± 22 °C (2σ error) for two samples from the Bear Lake locality using the garnet-biotite thermometer of Hodges and Spear (1982) and an assumed pressure of 350–400 MPa.

Eastern Bear Lake Subterrane

Banded Gneiss

The banded gneiss lies entirely within the mapped extent of the northern mylonite zone (Fig. 2). It is generally a mylonite, with a 50–100-m-wide band of ultramylonite at the contact with the French Slate. Mylonitic banded gneiss contains alternating 0.5–3-cm-wide, light-colored layers containing quartz + plagioclase + K-feldspar ± biotite ± epidote and 0.1–3-cm-wide, dark-colored layers containing plagioclase + K-feldspar + quartz + biotite + epidote + titanite + muscovite ± hornblende ± calcite. Ultramylonites are compositionally homogeneous. Both mylonites and ultramylonites contain strong, straight, northeast-striking, subvertical grain-shape foliations defined by flattened feldspar and quartz grains and aligned micas (Figs. 3B and 4A). Ultramylonites are S tectonites with no visible lineations on foliation surfaces. Mylonites are S to S > L tectonites. Where present, weakly developed mineral lineations in mylonites are defined by elongated quartz and feldspar grains and aggregates of biotite grains, and they range from subhorizontal to steeply plunging (Fig. 3B). In a few outcrops, foliation in mylonite is deformed by 10–30-cm-scale, moderately to steeply plunging, upright, tight-to-isoclinal folds.

Quartz in mylonites and ultramylonites exhibits sweeping undulose to straight extinction and few to no subgrains. Individual quartz grains are 50–500 µm in width, irregular or amoeboid in shape, and contain many embayments. Island quartz grains hosted in larger grains are common. Mylonites contain many 1–2-mm-wide feldspar porphyroclasts that display sweeping or patchy undulose extinction. Most feldspar grain boundaries in mylonites exhibit ~10 µm lobate sutures and irregularly shaped 10 µm neoblasts, and they locally display 10–25 µm subgrains that grade into partial rims of 10–25 µm neoblasts. Feldspar in ultramylonites is almost entirely recrystallized, with textures the same as those observed in mylonites.

Biotite Gneiss

The biotite gneiss is exposed in the southeastern third of the field area, and the northern part of this unit is cut by the northern mylonite zone (Fig. 2). Outside of the northern mylonite zone, the biotite gneiss consists of discontinuous bands, pods, and individual crystals of pink-weathering feldspar and quartz hosted in a relatively fine-grained black or charcoal gray matrix containing plagioclase + K-feldspar + quartz + biotite + epidote (Fig. 4B). A weak grain-shape

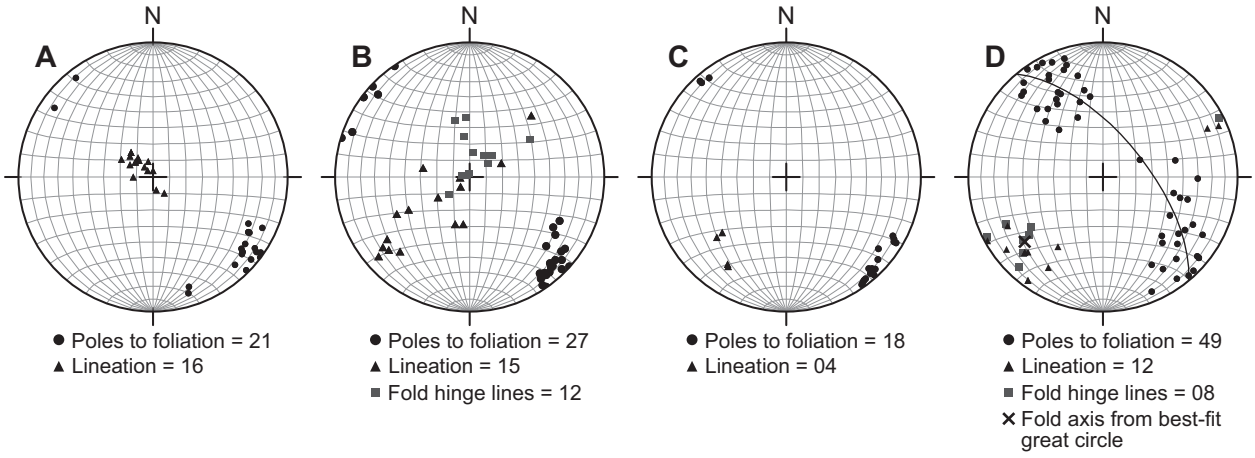

Figure 3. Orientations of foliations, lineations, and fold hinge lines measured in the Bear Lake locality. The plots are arranged from northwest to southeast, from left to right. (A) Orientations of foliations and lineations measured in the French Slate. (B) Orientations of foliations, lineations, and hinge lines of outcrop-scale folds measured in the banded gneiss. (C) Orientations of foliations and lineations measured in the biotite gneiss where it is cut by the northern mylonite zone. (D) Orientations of foliations, lineations, and hinge lines of outcrop-scale folds measured in the biotite gneiss outside of the northern mylonite zone. Note that the pole to the best-fit great circle to the poles to foliation is subparallel with the fold hinge lines and the lineations.

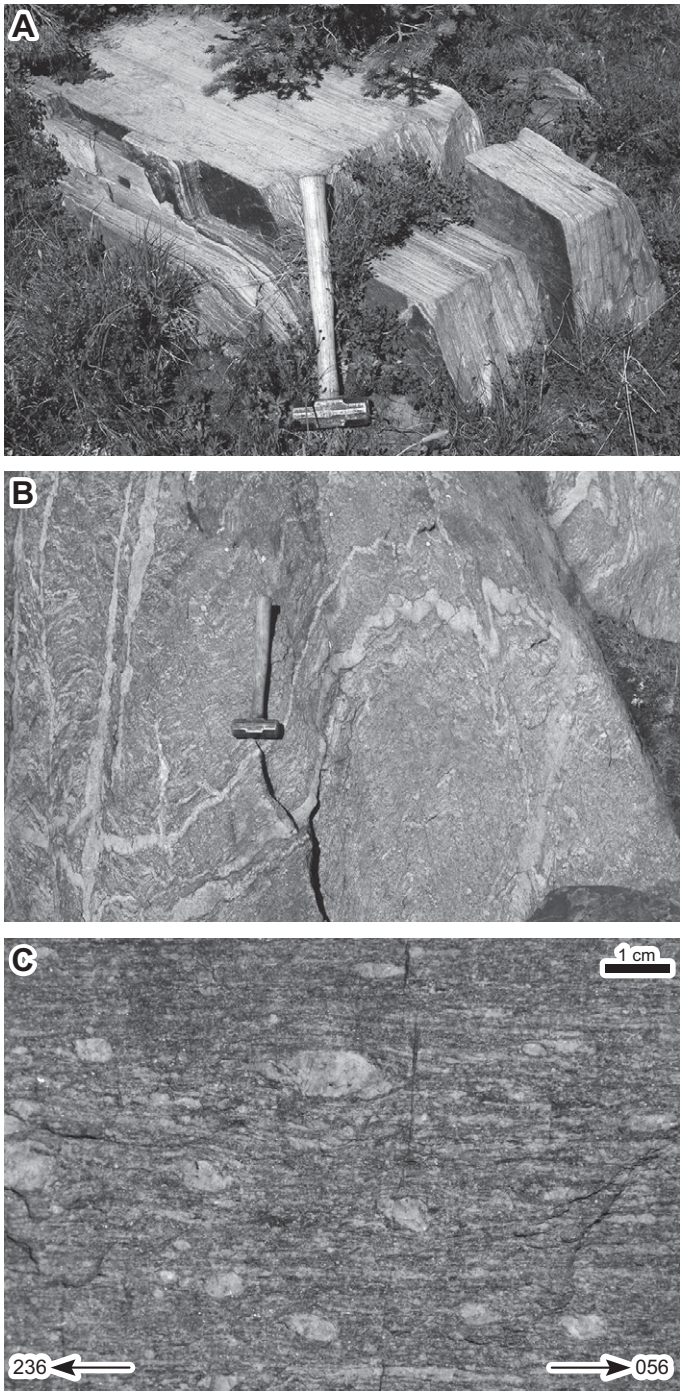

Figure 4. (A) Photograph of the banded gneiss at station CB72. View is toward the west. Note the strong, straight, northeast-striking, subvertical foliation. Hammer for scale is 36 cm long. (B) Photograph of the biotite gneiss outside of the northern mylonite zone at station CB191. View is toward the southwest. Note the discontinuous compositional segregation, deformed and undeformed granite dikes, and upright, gently southwest-plunging folds of the older generation of dikes. Hammer for scale is 36 cm long. (C) Photograph of the biotite gneiss cut by the northern mylonite zone at station CB193. View is straight down on a subhorizontal, foliation-perpendicular face. Note the asymmetrical feldspar porphyroclasts indicating sinistral strike-slip motion. Sample locations are given in Figure 2.

foliation is parallel with compositional layering. Layering and foliation in the biotite gneiss are deformed by gently southwest-plunging, moderately inclined to upright, open to tight, northwest- and southeast-vergent folds (Fig. 4B). The hinge zones of these folds contain subhorizontal to gently southwest-plunging mineral lineations defined by elongated and rodded quartzofeldspathic pods and individual feldspar and quartz grains (Fig. 3D); rocks in fold hinge zones are commonly L tectonites. Both local fold hinges and the regional fold axis defined by the best-fit great circle to the poles to foliations/layering are subparallel with the mineral lineations in the biotite gneiss (Fig. 3D). These folds tighten approaching the northern mylonite zone, and fold axial planes become parallel with the mylonitic foliation as gneissic banding is progressively transposed in the northern mylonite zone.

In the northern mylonite zone, the biotite gneiss is a relatively homogeneous mylonite with a strong, straight, northeast-striking, subvertical grain-shape foliation defined by aligned biotite and flattened feldspar and quartz grains (Fig. 3C). These rocks are primarily S tectonites with no visible lineations on foliation surfaces. Where weakly developed mineral lineations are present, they are gently plunging and defined by elongated quartz and feldspar grains. Conspicuous 2–15-mm-wide plagioclase and K-feldspar porphyroclasts are present in every outcrop of the mylonitic biotite gneiss (Fig. 4C). Mylonites of the biotite gneiss exhibit the same quartz and feldspar recrystallization textures as the mylonitic banded gneiss.

BEAR LAKE LOCALITY KINEMATIC ANALYSES

Meso- and Microstructural Analyses

Introduction and Methods

We conducted systematic kinematic analyses using microstructural and mesostructural kinematic indicators throughout the northern mylonite zone at the Bear Lake locality. We examined subhorizontal and subvertical, foliation-perpendicular faces throughout the field area. In samples CB195-B and CB196, we also analyzed faces at 45° to strike, dipping north, and 45° to strike, dipping south (Fig. 5). Kinematic indicators in these samples were classified as: (1) sinistral, symmetrical, or dextral in strike-parallel faces; (2) northwest-side-up/sinistral, symmetrical, and southeast-side-up/dextral in north-dipping faces; (3) northwest-side-up/dextral, symmetrical, and southeast-side-up/sinistral in south-dipping faces; and (4) northwest-side-up, symmetrical, or south-

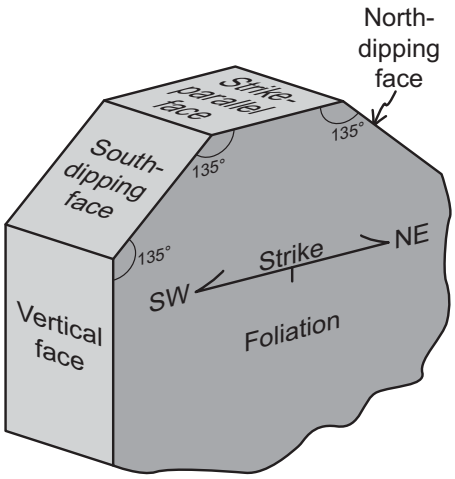

Figure 5. Cartoon showing how samples were cut in four different foliation-perpendicular directions. The traces of these cuts on the foliation are all 45° apart, and one of them must be within 22.5° of the transport direction. Figure is modified from Sullivan et al. (2011).

east-side-up in vertical faces. Unfortunately, none of these samples was suitable for more precise quantitative estimates of the degree of noncoaxial deformation (see review by Xypolias, 2010).

Results

In the French Slate, useful kinematic indicators include pressure-shadow overgrowths on garnet and biotite porphyroblasts (Fig. 6) (Simpson and Schmid, 1983; Etchecopar and Malavieille, 1987) and biotite fish formed from porphyroblasts without pressure-shadow overgrowths (ten Grotenhuis et al., 2003). The large majority of overgrowths and porphyroblasts in both lineation-parallel and lineation-perpendicular thin sections are symmetrical (Fig. 7). The lineation-perpendicular face of sample CB182 exhibits a significant population of sinistral kinematic indicators (Fig. 7). Otherwise, populations of asymmetrical kinematic indicators in these samples are quite small and evenly distributed.

In the banded gneiss mylonites, both quartz and feldspar deformed by pervasive crystal-plastic flow and are highly recrystallized. This limits the number of suitable kinematic indicators in this lithology, and most samples yielded little useful information. However, thin sections from two samples, CB196 and CB195-B, exhibit significant populations of tailed and tailless feldspar porphyroclasts (Figs. 8A and 8B) (Passchier and Simpson, 1986), bookshelf feldspars (Simpson and Schmid, 1983), shear bands (Fig. 8C) (Berthé et al., 1979; Platt and Vissers, 1980), and type-I S-C fabrics (Fig. 8D) (Berthé et al., 1979; Lister and Snoke, 1984). Strike-parallel faces of both CB196 and CB195-B contain no convincing kinematic indicators, and the majority of clast-based kinematic indicators from the other faces are symmetrical (Fig. 9). Vertical and dipping faces of these samples do exhibit significantly more northwest-side-up than southeast-side-up clast-based kinematic indicators (Fig. 9). These are the only faces that exhibit shear bands and local S-C fabrics, and these microstructures also indicate northwest-side-up motion (Figs. 8C and 8D).

In the biotite gneiss mylonites, quantitative kinematic data were collected in the field at five different stations using the conspicuous feldspar porphyroclasts (Figs. 2, 4C, and 10). Rocks at stations CB73, CB193, CB192, and CB67 are primarily S tectonites. Foliation faces at station CB199 contain gently southeast-plunging mineral lineations, and we analyzed a foliation-perpendicular, lineation-parallel exposure. There are no foliation-perpendicular, vertical exposures at station CB199. A large majority of clasts visible in all of the subhorizontal exposures of the biotite gneiss exhibit sinistral asymmetry (Fig. 10). A majority of clasts exposed on subvertical faces are symmetrical, and the populations of asymmetrical clasts are evenly distributed (Fig. 10).

Quartz Crystallographic Fabric Analyses

Methods

Quartz crystallographic fabrics were measured in samples CB174 and CB65 (Fig. 2) by collecting electron backscatter diffraction (EBSD) patterns. These were acquired with a scanning electron microscope (SEM) at Bowdoin College equipped with an HKL Nordlys II detector and Channel 5 software (software details in Schmidt and Olesen, 1989). Samples were prepared by polishing microprobe-polished thin sections approximately four additional hours in a noncrystallizing colloidal silica suspension on a vibratory polisher (SYTON method of Fynn and Powell, 1979). The thin sections were not carbon coated; charging was minimized by using a chamber pressure of 15 Pa combined with the 70° tilt required for pattern acquisition. Operating parameters were an accelerating voltage of 20 kV, a working distance of 25 mm, and a beam current of 2.2 nA. Channel 5 acquisition and indexing settings were 4 × 4 binning, high gain, 7 frames averaged, Hough resolution = 65, 6 bands, and 85 reflectors. Quartz was indexed using the lattice parameters of Sands (1969). Accepted data points were limited to those with mean angular

Figure 6. Photomicrograph of a garnet porphyroclast with symmetrical quartz pressure-shadow overgrowths in CB183. The thin section is cut parallel with the downdip lineation and perpendicular to the steeply dipping foliation, and the view is toward the northeast in geographic coordinates. Plane polarized light. Sample location given in Figure 2.

deviations less than 1° based on the number of bands (6) detected compared to the experimental work of Krieger-Lassen (1996) on the precision of crystal orientations. EBSD patterns were collected in an automated mapping mode with step sizes of 3 µm for CB65 and 10 µm for CB174, which allowed collection of tens of data points per grain. Grains were grown to completion using an iterative extrapolation routine in which nonindexed data points acquired the average orientation of six neighbors. Prior et al. (2009) demonstrated that this method does not create substantial artifacts. The data were further processed to define grains, and grains defined by this routine that were less than 60 µm in diameter were removed (method of Prior et al., 2009). One averaged point per grain is plotted on the stereonets in Figure 11.

Results

Sample CB174 is a mylonitic micaceous quartzite hosted in the French Slate near the terrane-bounding fault zone (Fig. 2). This sample is an S tectonite. The crystallographic fabric data were collected from a thin section made from a vertical cut (Figs. 11A and 11C). The *a*-axis maxima lie at the plot margins, and the central girdle of the *c*-axis fabric passes through the plot center when the data are viewed in a north-dipping, foliation-perpendicular plane that is 51° from strike (Figs. 11B and 11C). In

this reference frame, the *c* axes define a kinked single girdle passing through the center of the plot, and the *a* axes define two maxima at the plot margins connected by a single diffuse small-circle girdle (Figs. 11B and 11C).

Sample CB65 is an ultramylonite of the banded gneiss collected 40 m across strike from the contact with the French Slate (Fig. 2). This sample is also an S tectonite. Crystallographic fabric data were collected from a 1-mm-wide quartz vein in a thin section made from a strike-parallel cut (Figs. 11D and 11F). The *a*-axis maxima lie at the plot margins when the data are viewed in a south-dipping plane 70° from strike (Figs. 11E and 11F). In this reference frame, the *c*-axis fabric forms a partial asymmetrical cross girdle that is not connected in the plot center, and the *a* axes define weak maxima at the plot margins connected by diffuse small-circle girdles (Figs. 11E and 11F).

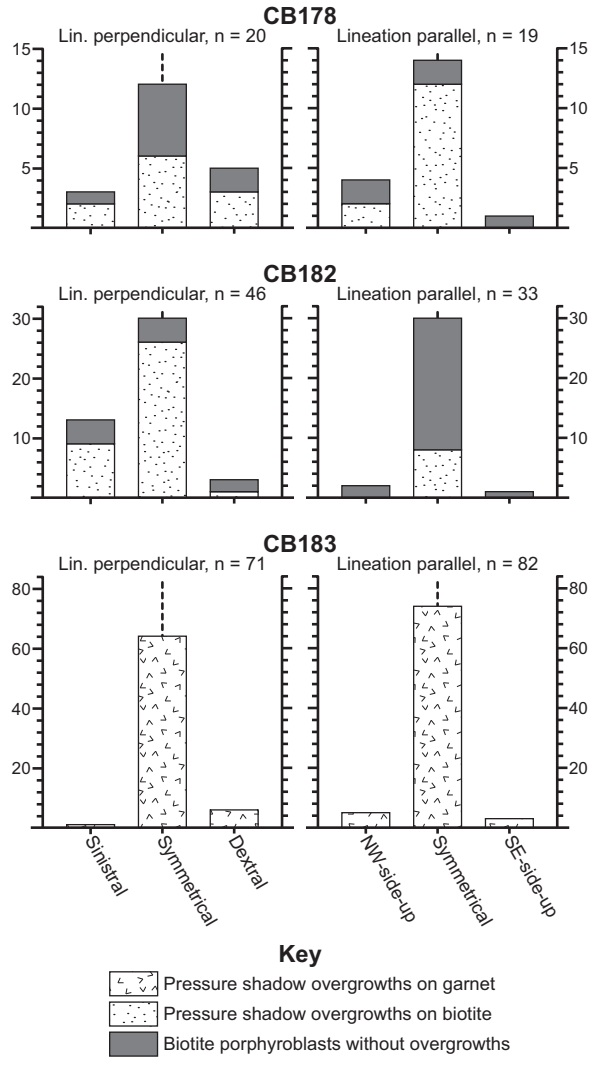

Figure 7. Microstructural kinematic analyses of biotite and garnet porphyroblasts in the French Slate cut by the northern mylonite zone in the Bear Lake locality. Station locations are given in Figure 2. All faces are cut perpendicular to the foliation. Lineations in these samples plunge straight down the dip of the foliation; hence, lineation-parallel cuts are essentially vertical.

INTERPRETATION OF THE BEAR LAKE LOCALITY

Deformation Temperatures

French Slate

In the Bear Lake locality, the French Slate contains the prograde assemblage garnet + biotite + muscovite ± chlorite that records metamorphism under upper-greenschist- or lower-amphibolite-facies temperatures (Spear and Cheney, 1989; Spear, 1993). Because these minerals define the foliation and lineation, deformation probably took place under these temperature conditions. The temperatures of 433 ± 18 °C and 449 ± 22 °C calculated by Duebendorfer (1988) are probably minimum values, because there is evidence for retrograde metamorphism in all of the samples in his study (Duebendorfer, 1988). Therefore, the French Slate in the Bear Lake locality probably records deformation at temperatures of 430–500 °C.

Eastern Bear Lake Subterrane

Dynamic recrystallization of quartz and feldspar is sensitive to variations in temperature, and the microscopic textures of these minerals can be used to estimate deformation temperatures in plastically deformed rocks (Tullis and Yund, 1987; Hirth and Tullis, 1992; Stipp et al., 2002a). Rocks of the eastern Bear Lake subterrane cut by the northern mylonite zone exhibit similar quartz and feldspar recrystallization textures throughout the field area. These textures indicate that quartz in mylonites and ultramylonites underwent fast grain-boundary-migration dynamic recrystallization, and feldspar underwent simultaneous grain-boundary-bulging and minor subgrain-rotation dynamic recrystallization. Assuming typical geologic strain rates of 10^{-13} to 10^{-14}, deformation temperatures recorded by these samples are greater than 500 °C and less than 650 °C (Tullis and Yund, 1987; Hirth and Tullis, 1992; Stipp et al., 2002a).

Wall-Rock Deformation

We agree with Duebendorfer and Houston (1986, 1987) and interpret the upright folds in the biotite gneiss outside of the northern mylonite zone as coeval with the Cheyenne belt shear zones. The gneissic foliation in this unit must at least partially predate this folding because it is deformed in fold hinge zones. Since these rocks are probably Archean in age (Ball and Farmer, 1991), this fabric could be Archean. The rotated gneissic foliation in the fold limbs likely records some Paleoproterozoic horizontal shortening, and possibly flattening strain, as most of the unit is an S tectonite. The L tectonites in the hinge zones of these folds probably formed via penetrative horizontal shortening of the preexisting subhorizontal gneissic foliation in the fold hinge zones (cf. Sullivan, 2013, his fig. 9).

Meso- and Microstructural Kinematic Indicators

Field studies and models of transpressional shear zones show that simple-shear–dominated deformation can result in flattening strains or mineral elongation lineations that are highly oblique or even perpendicular to the slip direction (e.g., Sanderson and Marchini, 1984; Fossen and Tikoff, 1993; Greene and Schweickert, 1995; Dutton, 1997; Dewey et al., 1998; Jiang and Williams, 1998; Czeck and Hudleston, 2003; Jones et al., 2004; Kuiper et al., 2011). Careful structural analyses of multiple sample orientations can constrain the slip direction in such shear zones (e.g., Greene and Schweickert, 1995; Tikoff and Greene, 1997; Czeck and Huddleston, 2003; Giorgis and Tikoff, 2004;

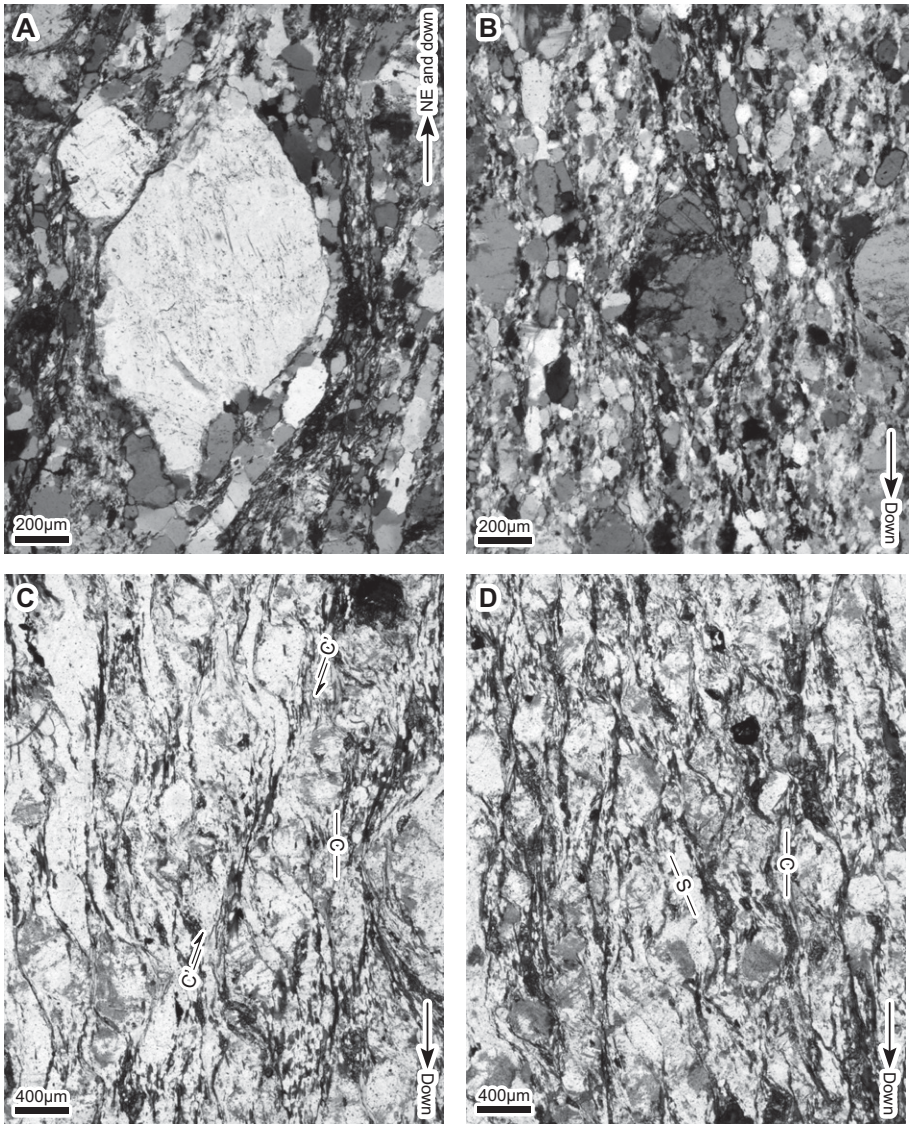

Figure 8. Photomicrographs of kinematic indicators in samples of the banded gneiss, CB196 and CB195-B. Arrows along the right-hand sides of the images depict geographic coordinates. (A) Asymmetrical feldspar porphyroclast indicating northwest-side-up, sinistral, oblique-slip motion. The thin section was made from the north-dipping cut of CB195-B, and the view is down into the ground and toward the southwest in geographic coordinates. Parallel polarized light. (B) Symmetrical feldspar porphyroclast indicating coaxial horizontal shortening. The thin section was made from the vertical cut of CB196, and the view is toward the northeast in geographic coordinates. Parallel polarized light. (C) Shear band indicating northwest-side-up, dip-slip motion. The thin section was made from the vertical cut of CB195-B, and the view is toward the northeast in geographic coordinates. Plane polarized light. (D) S-C fabrics indicating northwest-side-up motion. The thin section was made from the vertical cut of CB195-B, and the view is toward the northeast in geographic coordinates. Plane polarized light.

Sullivan and Law, 2007; Sullivan et al., 2011). In these shear zones, the face with the most numerous and most internally consistent kinematic indicators, or the face with the greatest asymmetry, should be nearest to parallel with the transport direction.

Meso- and microstructural kinematic indicators throughout the northern mylonite zone indicate that there was significant strain partitioning between rock units. Most potential kinematic indicators from French Slate samples CB178, CB182, and CB183 are symmetrical on horizontal and vertical faces. Hence, most of this unit probably experienced strongly coaxial deformation that accommodated foliation-normal shortening and vertical elongation. The sinistral kinematic indicators in CB182 indicate that the French Slate also records some localized sinistral strike-slip motion, in present-day coordinates. In the mylonitic banded gneiss, the large number of symmetrical clasts and the presence of shear bands indicate significant coaxial shortening. The populations of asymmetrical kinematic indicators in dipping and vertical faces of CB196 and CB195-B also indicate that mylonitic fabrics in this unit probably accommodated some northwest-side-up, dip-slip motion, in present-day coordinates. In the mylonitic biotite gneiss, horizontal exposures consistently exhibit majority populations of asymmetrical sinistral kinematic indicators, and the lineation-parallel exposure at CB199 exhibits the greatest asymmetry of any face examined. Fabrics on vertical exposures are generally symmetrical. Therefore, mylonitic fabrics in this unit probably record simple-shear–dominated deformation that accommodated sinistral strike-slip motion, in present-day coordinates.

Crystallographic Fabrics

Quartz crystallographic fabric formation and the resulting fabric geometries are sensitive to variations in the noncoaxiality of flow (e.g., Lister and Hobbs, 1980; Schmid and Casey, 1986; Law et al., 1990) and distortional strain geometry (e.g., Lister and Hobbs, 1980; Law, 1986; Schmid and Casey, 1986; Sullivan and Beane, 2010). The three most important crystallographic slip systems in naturally deformed quartzites at temperatures that range from the onset of crystal plasticity to ~650 °C are basal ⟨a⟩, rhomb ⟨a⟩, and prism ⟨a⟩ (Schmid and Casey, 1986; Stipp et al., 2002b). As quartz crystallographic fabrics form under these temperature conditions, the *a*-axis maxima track the transport direction (slip vector) during simple-shear–dominated deformation or form conjugate pairs or girdles around the maximum or minimum elongation directions during coaxial deformation (Schmid and Casey, 1986; Sullivan and Beane, 2010). Therefore, by placing them in a geographic reference frame, quartz *a*- and *c*-axis fabrics can constrain the external kinematic framework imposed on a sample (Wallis, 1992; MacCready, 1996; Sullivan and Law, 2007).

In the French Slate sample, CB174, the *a*-axis maxima lie at the plot margins, and the central girdle of the *c*-axis fabric passes through the plot center when the data are viewed in a north-dipping, foliation-perpendicular plane that is 51° from strike (Figs. 11B and 11C). This plane

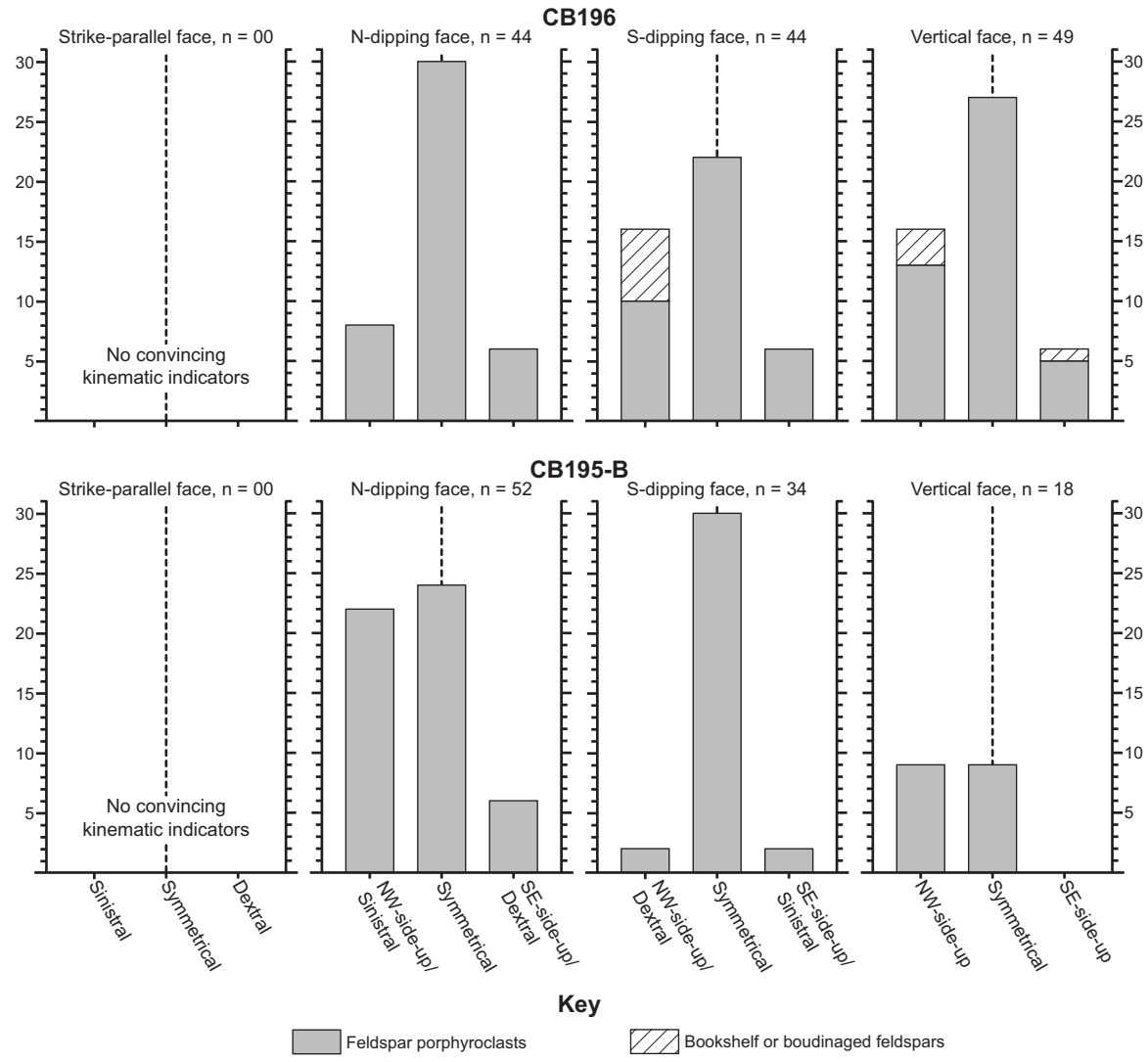

Figure 9. Microstructural kinematic analyses of feldspar porphyroclasts and bookshelf feldspar grains in the banded gneiss cut by the northern mylonite zone in the Bear Lake locality. Station locations are given in Figure 2. All faces are cut perpendicular to the foliation. The deformation fabric appears less intense when viewed in the strike-parallel faces, and no convincing kinematic indicators were observed in these thin sections.

is roughly parallel with the transport direction recorded by this sample. The asymmetry of the *c*-axis fabric and the *a*-axis maxima indicate simple-shear–dominated deformation that accommodated northwest-side-up, sinistral oblique-slip, motion. The *a*-axis fabric also defines a weak small-circle girdle about the pole to the foliation in one half of the plot, and this indicates a small component of coaxial flattening (Schmid and Casey, 1986).

In the ultramylonitic banded gneiss sample, CB65, the *a*-axis maxima lie at the plot margins when the data are viewed in a south-dipping plane 70° from strike (Figs. 11E and 11F). This plane is roughly parallel with the transport direction recorded by this sample. The asymmetry of the *c*-axis fabric and the *a*-axis maxima indicate southeast-side-up, sinistral oblique-slip motion. The absence of *c* axes in the center of the plot, the presence of a small-circle girdle of *c* axes in one half of the plot, and the diffuse *a*-axis girdle in one half of the plot also indicate a significant component of horizontal coaxial flattening (Lister and Hobbs, 1980; Law, 1986; Schmid and Casey, 1986).

Integrated Interpretation of the Bear Lake Locality

Rocks cut by the northern mylonite zone in the Bear Lake locality record a complex deformation geometry with a great deal of strain partitioning. From southeast to northwest, plastic deformation accommodated sinistral strike-slip motion; northwest-side-up, dominantly dip-slip motion; southeast-side-up, dominantly dip-slip motion; northwest-side-up, sinistral oblique-slip motion; and strongly coaxial, horizontal shortening with local subordinate sinistral strike-slip motion (Fig. 12). We interpret the mylonitic fabrics in the biotite gneiss, banded gneiss, and French Slate as coeval for three reasons: (1) Mylonitic foliations in these domains are all subparallel; (2) they formed under similar temperature conditions; and (3) they are all kinematically related with evidence for sinistral strike-slip; northwest-side-up, dip-slip; sinistral/northwest-side-up, oblique-slip motion; and ubiquitous coaxial horizontal shortening. These mylonitic fabrics effectively accommodate sinistral, northwest-side-up oblique transpression. We

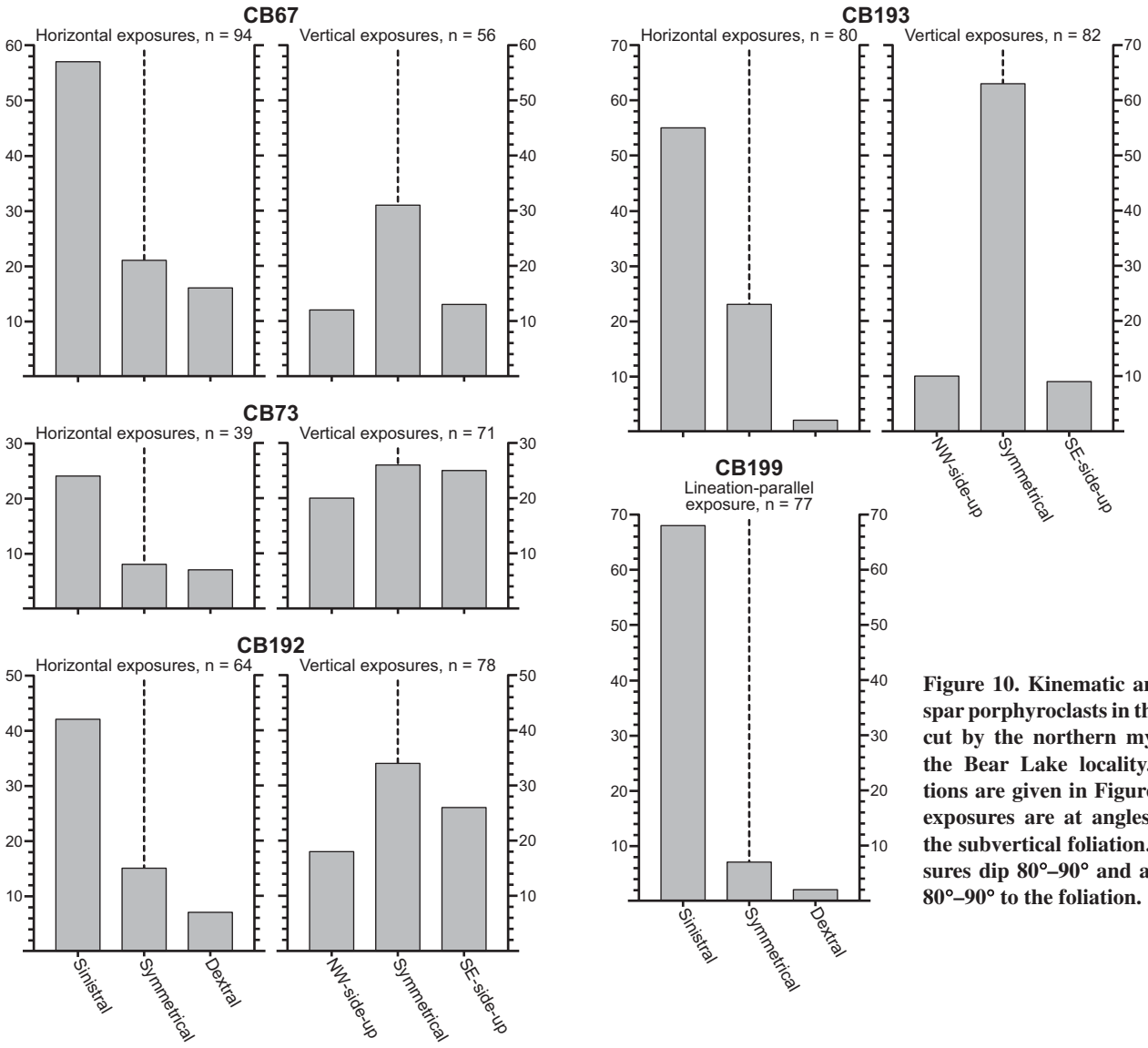

Figure 10. Kinematic analyses of feldspar porphyroclasts in the biotite gneiss cut by the northern mylonite zone in the Bear Lake locality. Station locations are given in Figure 2. Horizontal exposures are at angles of 80°–90° to the subvertical foliation. Vertical exposures dip 80°–90° and are at angles of 80°–90° to the foliation.

interpret the 50–100-m-wide ultramylonite zone cutting the banded gneiss at the terrane boundary as a younger feature because it is kinematically distinct (southeast-side-up motion), and because the presence of a relatively narrow band of ultramylonite fabrics at the terrane boundary implies late-phase strain localization.

ADDITIONAL EVIDENCE FOR SINISTRAL MOTION IN THE CHEYENNE BELT

Observations

At least two additional areas in the Cheyenne belt record sinistral strike-slip motion—the Bear Mountain and Middle Fork localities (Fig. 1). The Bear Mountain locality is located in the southeastern Sierra Madre where the southernmost strand of the Cheyenne belt is exposed just north of Bear Mountain (Fig. 1). Exposure is poor in this area, but a single large outcrop along the ridge approaching Bear Mountain enabled a quantitative kinematic analysis. The shear zone here cuts metagabbro of the Green Mountain terrane that was intruded by numerous coarse-grained to pegmatitic leucogranite dikes (Houston and Graff, 1995; Jones et al., 2010). The mafic rocks are S tectonites with strong, straight, east-striking, subvertical foliations defined by greenschist-facies minerals; and the granite dikes are extensively boudinaged (Fig. 13). Sixty-three granite boudins are exposed in subhorizontal faces in this outcrop. Forty-one of these exhibit sinistral asymmetry, 20 are symmetrical, and 2 exhibit dextral asymmetry. Thirty-three boudins are exposed in subvertical, foliation-perpendicular faces. Eight of these indicate north-side-up motion, 21 are symmetrical, and 4 boudins indicate south-side-up motion.

The Middle Fork locality is an exposure of the southern mylonite zone near the Middle Fork of the Little Laramie River in the eastern Medicine Bow Mountains (Fig. 1). Here, the southern mylonite zone consists of a number of subparallel high-strain zones previously interpreted as an anastomosing shear zone network (Duebendorfer and Houston, 1987; Duebendorfer, 1990). The central strand of these shear zones is a 20–100-m-wide mylonite/ultramylonite zone. The boundaries of this zone are abrupt, and it contains northeast-striking, steeply southeast-dipping foliations and moderately to steeply northeast-plunging mineral lineations. Microstructural kinematic indicators observed on foliation-perpendicular, lineation-parallel faces in the main mylonite/ultramylonite zone

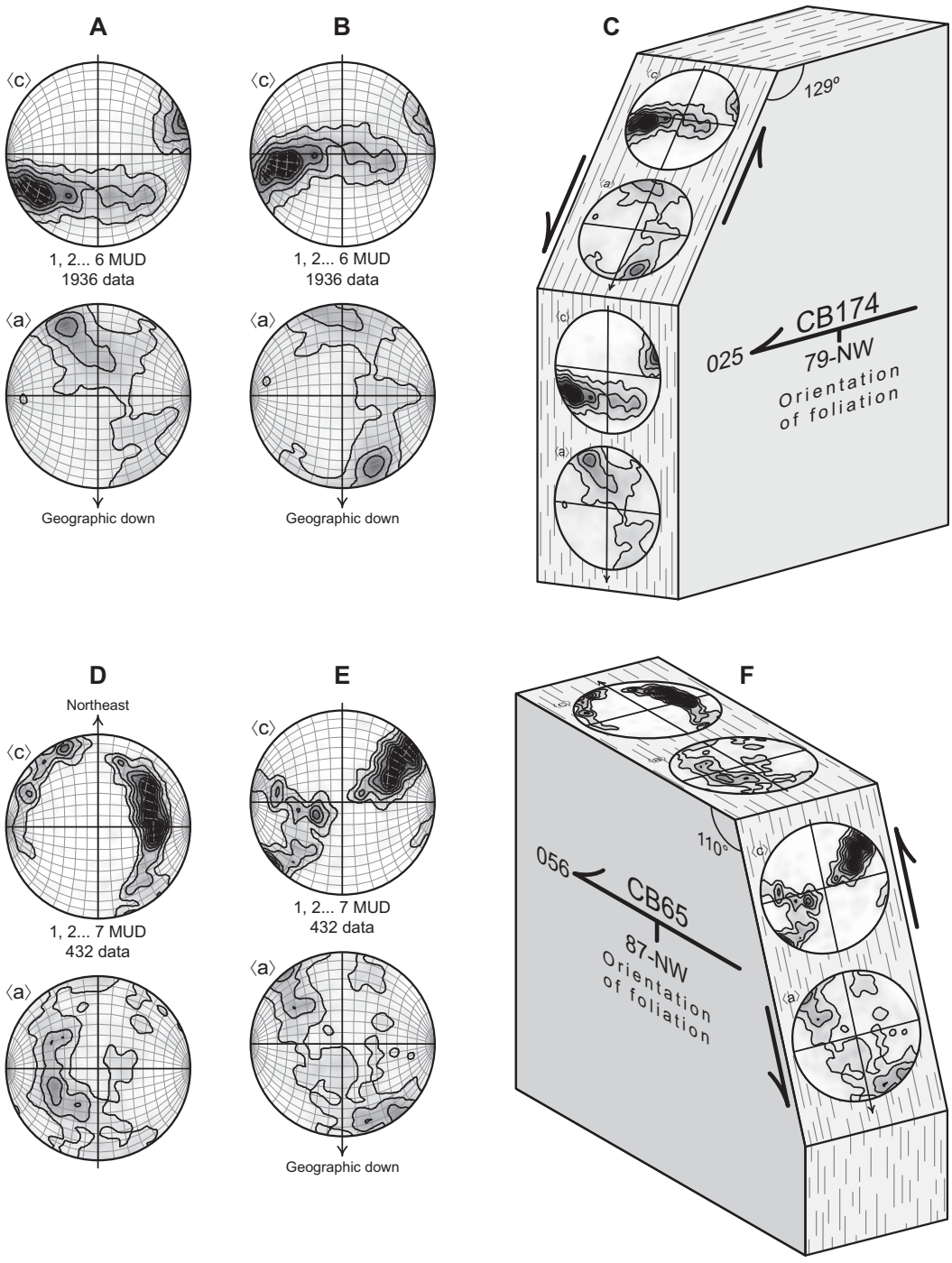

Figure 11. Quartz crystallographic fabric data plotted on equal-area, lower-hemisphere projections with the foliation lying along the north-south great circles of the plots. Contours are multiples of uniform density (MUD). Sample locations given in Figure 2. (A) Data from CB174 viewed as collected in a foliation-perpendicular, vertical plane looking toward the southwest in geographic coordinates. (B) Data from CB174 rotated 39° about the pole to the foliation so that the *a*-axis maxima lie at the plot margins, and the central girdle of the *c*-axis fabric passes through the plot center. This projection plane is parallel with the transport direction, and it is 51° from strike and dips toward the northeast in geographic coordinates. (C) Cartoon oriented sample illustrating the geometric relationship between the data viewed in A and B in geographic coordinates. (D) Data from CB65 viewed as collected in a foliation-perpendicular, strike-parallel plane looking down into the ground. (E) Data from CB65 rotated 70° about the pole to the foliation so that the *a*-axis maxima lie at the plot margins, and the central girdle of the *c*-axis fabric passes through the plot center. This projection plane is parallel with the transport direction, and it is 70° from strike and dips toward the southwest in geographic coordinates. (F) Cartoon oriented sample illustrating the geometric relationship between the data viewed in D and E in geographic coordinates.

overwhelmingly indicate southeast-side-up, dominantly dip-slip motion; other faces reveal much less asymmetry. Both quartz and feldspar in the central zone deformed plastically. The central mylonite/ultramylonite zone is flanked by numerous 5–50-m-wide mylonite/protomylonite zones. The flanking zones have gradational boundaries and contain northeast-striking, subvertical foliations (Duebendorfer, 1986, 1990). Most of the mylonite/protomylonite zones exhibit sinistral type I S-C fabrics (Lister and Snoke, 1984) on subhorizontal faces and subhorizontal, ridge-in-groove–style ductile slicken lineations (Lin and Williams, 1992) on the subvertical C surfaces. Duebendorfer (1986) reported steeply plunging lineations on S surfaces in these rocks. Quartz and feldspar both deformed plastically in these S-C tectonites, and they exhibit similar recrystallization textures in both S and C domains.

Interpretations

The data from the Bear Mountain locality closely match the results from the mylonitic biotite gneiss of the Bear Lake locality. These rocks probably record simple-shear–dominated deformation that accommodated sinistral strike-slip motion, in present-day coordinates.

The main mylonite/ultramylonite zone in the Middle Fork locality accommodated southeast-

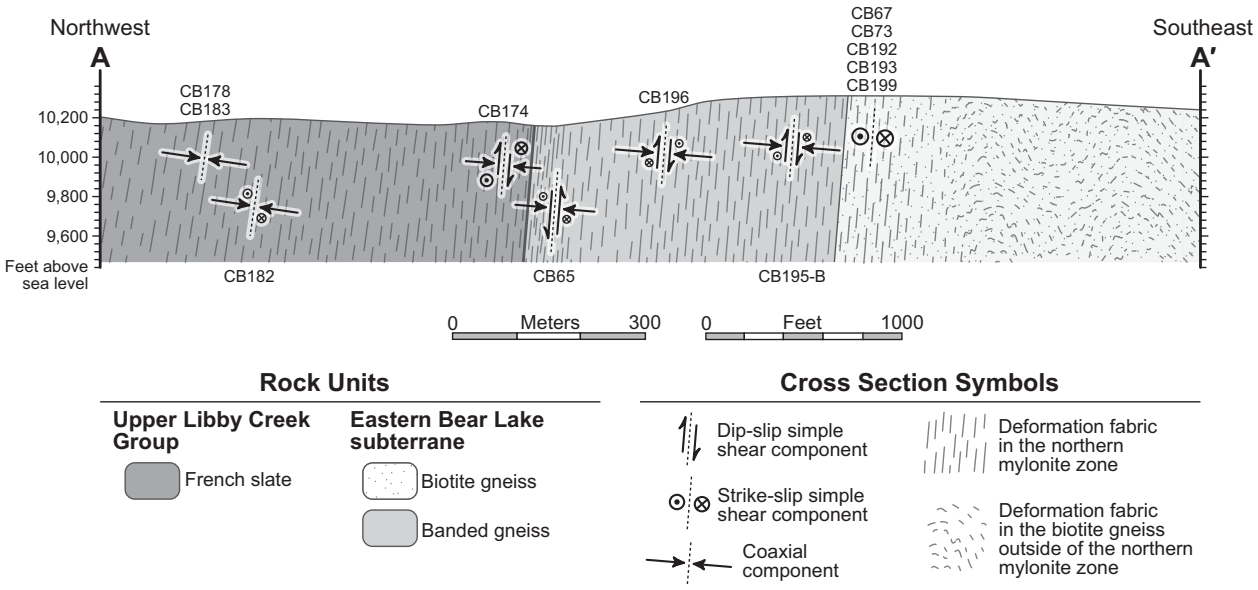

Figure 12. Schematic cross section through the northern mylonite zone along line A–A′ in Figure 2. The arrows represent the different deformation components deduced from the outcrop and thin-section–based kinematic analyses, and the quartz crystallographic fabric analyses.

side-up, dip-slip motion, and the flanking shear zones record sinistral strike-slip motion. Duebendorfer (1986) interpreted the sinistral S-C fabrics in the flanking zones as polyphase features based on his observation of two lineations. We see no field or microstructural evidence for two deformation events, and quartz and feldspar exhibit similar recrystallization textures in both S and C domains. This indicates that the S and C domains are coeval. The doubly lineated rocks observed by Duebendorfer (1986) are easily explained by strain partitioning between S and C domains, wherein S domains accommodated more horizontal shortening and vertical elongation, and C domains accommodated sinistral strike-slip motion (cf. Tikoff and Greene, 1997). Exposure is limited in the Middle Fork locality, and we did not observe crosscutting relationships between the flanking mylonite/protomylonite zones and the main mylonite/ultramylonite zone. However, our preferred interpretation of this area is that the central mylonite/ultramylonite zone represents late-phase strain localization dominated by southeast-side-up motion, and the flanking mylonite/protomylonite zones record an earlier phase of sinistral strike-slip motion, in present-day coordinates.

INCORPORATION INTO THE REGIONAL FRAMEWORK

Evidence for sinistral strike-slip motion, in present-day coordinates, is found at the three localities described in this paper. It also is indicated by the sinistral separation of horses of lower Libby Creek Group rocks cut off from the French Creek syncline, and the geometry of the syncline itself implies drag folding along a sinistral fault zone (Houston and Karlstrom, 1992). However, Sullivan et al. (2011) found no significant evidence for sinistral strike-slip motion in two similar detailed investigations in the western Medicine Bow Mountains (Fig. 1). There are two possible explanations for the discontinuous nature of evidence for sinistral motion along the Cheyenne belt: (1) Sinistral strike slip was discontinuous and localized in discrete domains; or (2) sinistral strike slip represents an earlier phase of deformation that was largely overprinted by later southeast-side-up, dip-slip motion. We favor the latter hypothesis for two reasons. First, there is no evidence for sinistral strike-slip motion where the Cheyenne belt narrows to a single 500-m-wide deformation zone in the western Medicine Bow Mountains (Fig. 1) (Sullivan et al., 2011). This prohibits continuity between strike-slip motion in the eastern Medicine Bow Mountains at the Bear Lake and Middle Fork localities and strike-slip motion in the eastern Sierra Madre at the Bear Mountain locality. Second, in both the Bear Lake and Middle Fork localities, southeast-side-up, dip-slip motion is confined to localized ultramylonite/mylonite zones, whereas evidence for sinistral strike-slip motion appears in less intensely deformed mylonites and protomylonites flanking the ultramylonites. This relationship indicates that the less intensely deformed rocks record an earlier phase of deformation that was overprinted by the localized ultramylonite/mylonite zones. However, no overprinting relationships were observed in the field.

Figure 13. Photograph of an asymmetrical granite boudin at the Bear Mountain locality, eastern Sierra Madre (see Fig. 1 for location). Subhorizontal exposure is viewed straight down into the ground, perpendicular to the subvertical foliation. The 14.5-cm-long pencil is parallel with the foliation, and its tip points toward 088°.

Three lines of evidence indicate that sinistral strike-slip and oblique-slip motion across the Cheyenne belt took place at ca. 1750 Ma. First, the rock unit cut by the Cheyenne belt in the Bear Mountain locality contains zircon with 1743 ± 14 Ma metamorphic overgrowths (Jones et al., 2010), and deformation in this zone postdates peak metamorphism. Second, the boudinaged granite dikes at the Bear Mountain locality are correlated with the ca. 1763 Ma synextensional Sierra Madre granite (Jones et al., 2010). Third, S-C mylonites in the Middle Fork locality deform two-mica granite that is probably coeval with ca. 1748 Ma prograde metamorphism of the Barber Lake terrane (Duebendorfer, 1986; Duebendorfer and Houston, 1987; Strickland, 2004). Regardless of its exact age, sinistral, northwest-side-up, oblique-slip motion must have been coeval with the formation of the metamorphic gradient in the French Slate because synmetamorphic fabrics in the French Slate record sinistral strike-slip and sinistral, northwest-side-up, oblique-slip motion. This indicates that sinistral oblique transpression was the dominant deformation style along the Cheyenne belt in the eastern Medicine Bow Mountains and may have been the dominant deformational style throughout the belt.

MODELS FOR THE CHEYENNE BELT

Thrust Fault Model

Presently, the most widely accepted model for the region envisions the Cheyenne belt as a low-angle, crustal-scale thrust fault system rotated into its present subvertical orientation during late-stage, orogen-scale folding (Karlstrom and Houston, 1984; Duebendorfer and Houston, 1986, 1987; Duebendorfer, 1988). However, the new evidence for sinistral strike-slip motion across the Cheyenne belt does not agree with the thrust fault model (Table 1). Three lines of regional evidence are also incompatible with predictions inherent to the existing thrust fault model (Table 1). First, the French Slate at the northern margin of the Cheyenne belt (the presumptive footwall in the thrust model) records only low to moderate metamorphic pressures (Duebendorfer, 1988). Rocks buried beneath thrust sheets that were at temperatures of 650 °C or more during thrusting should record much higher metamorphic pressures. Second, metamorphosed mafic rocks exposed south of the Cheyenne belt contain amphibolite-facies mineral assemblages over 30 km across orogenic strike (Houston et al., 1968; Houston et al., 1989). Hence, there is no evidence for the gently dipping back limb of an orogen-scale fold or a progressive upward decrease in metamorphic grade in the hanging wall of the proposed thrust system. Finally, Paleoproterozoic deformational features throughout the central and southern Medicine Bow Mountains indicate penetrative horizontal shortening rather than nappe-style thrust faulting. For example:

(1) The French Slate resembles a classic slate belt with strong, straight, subvertical phyllitic foliations and isoclinal folds that indicate penetrative horizontal shortening (Houston et al., 1968; Karlstrom and Houston, 1984).

(2) Open to tight folds in the Bear Lake and Barber Lake terranes are upright and generally symmetrical (Duebendorfer and Houston, 1986, 1987).

(3)Amphibolite-facies foliations and lithologic contacts south of the Cheyenne belt are northeast striking and subvertical over 30 km across orogenic strike (Houston et al., 1968; Houston et al., 1989).

Based on these observations, we believe the existing data do not agree with the classic thrust fault model, wherein the main phase of deformation of the Cheyenne belt took place before the shear zones reached their present-day subvertical orientation.

Revised Model for the Cheyenne Belt

The Model

We propose the following revised model for the evolution of the Cheyenne belt that is largely built around the plate tectonic framework of Jones et al. (2010):

(1) The Paleoproterozoic record begins with 2400–2000 Ma rifting of the Wyoming craton, followed by formation of a passive margin along the southern edge of the Wyoming Province (Fig. 14A) (Karlstrom and Houston, 1984; Premo and Van Schmus, 1989). The protolith of the Barber Lake terrane may have been deposited concurrently with the Libby Creek Group in the tectonic basin between the Wyoming Province and the Green Mountain arc (Ball and Farmer, 1991; Jones et al., 2010). The Green Mountain arc formed as either: (1) a north-facing arc on a separate tectonic plate (Jones et al., 2010, their model 1); or (2) a south-facing arc built on a rifted fragment of the Wyoming Province and separated from it by a backarc basin (Jones et al., 2010, their model 2).

(2) The Snowy Pass Supergroup and supracrustal rocks of the Green Mountain terrane exposed in the western Sierra Madre were metamorphosed at ca. 1780 Ma (Duebendorfer et al., 2006). This metamorphism roughly coincides with the ca. 1774 Ma cessation of subduction-related magmatism in the Green Mountain terrane (Jones et al., 2010), and we attribute it to the initial tectonic juxtaposition of the Green Mountain terrane and the Wyoming Province (see Fig. 14B). This could have involved either a "soft hit" arc-continent collision (Jones et al., 2010, their model 1) or collapse of a backarc basin behind a fringing arc in response to shallowing of the subduction angle (Jones et al., 2010, their model 2). There are no constraints on the exact timing of the initial telescoping of the terranes in the Medicine Bow Mountains. We attribute it to largely thin-skinned deformation during this ca. 1780 Ma event, because the faults that cut the Snowy Pass Supergroup are deformed by the French Creek syncline, and both the syncline and the faults are truncated by the Cheyenne belt (Fig. 1) (Houston et al., 1968; Karlstrom and Houston, 1984; Houston and Karlstrom, 1992). These relationships imply two distinct kinematic phases. This deformation is represented by a thrust stack in Figure 14B, but it could have been transpressional. Faults formed during this phase of deformation probably created the crustal weak zones that later evolved into the Cheyenne belt shear zones.

(3) Postarc extension is recorded by ca. 1769–1759 Ma bimodal magmatism documented in the Sierra Madre (see Fig. 14C) (Jones et al., 2010). The undated bimodal intrusive rocks of the western Bear Lake subterrane may have formed during this event, but no evidence for this extensional episode has been recognized north of the Cheyenne belt. This magmatic pulse probably helped maintain a high thermal gradient in the Green Mountain terrane.

(4) Oblique plate convergence resulted in significant crustal contraction around 1750 Ma (Strickland, 2004; Duebendorfer et al., 2006; Jones et al., 2010). This drove amphibolite-facies metamorphism and penetrative crustal shortening in the young, hot, rheologically weak rocks south of the Cheyenne belt. Buttressing of this deformation against the old, cold, rheologically strong Archean basement caused earlier fault zones to steepen and become the subvertical Cheyenne belt shear zones. This was accompanied by reactivation and rotation of the faults cutting the Snowy Pass Supergroup (see Fig. 14D). In this model, the Cheyenne belt is a sinistral oblique transpressional stretching fault system (Means, 1989) that simultaneously accommodated sinistral strike-slip motion, horizontal shortening, and dip-slip motion related to differential vertical elongation between the Green Mountain terrane and the Wyoming Province. This resulted in bulk sinistral oblique-slip motion across the belt. The Bear Lake and Barber Lake terranes came from outside of the plane of section in Figure 14D, and there are no constraints

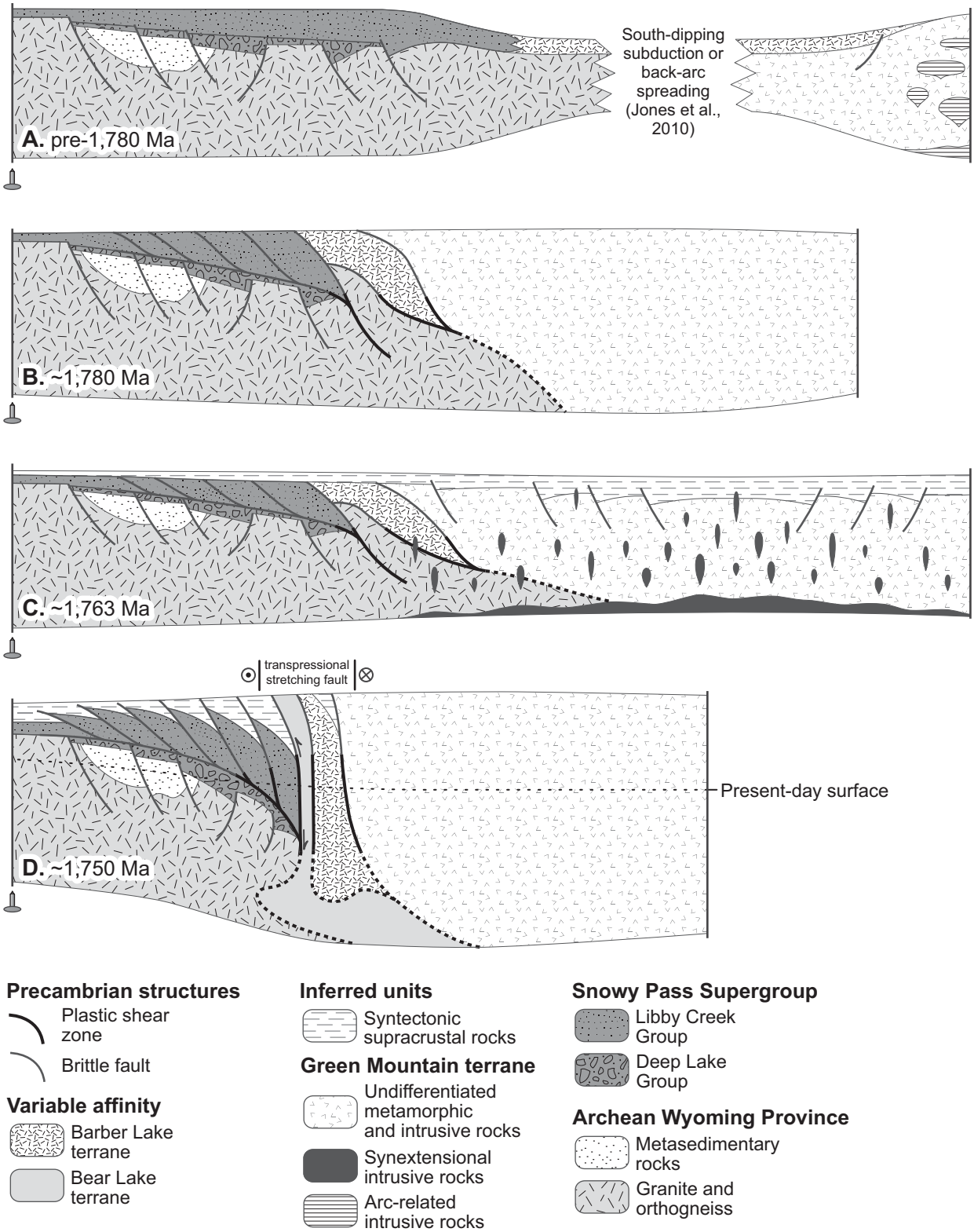

Figure 14. Cartoon depicting the Paleoproterozoic plate-tectonic and structural evolution of the Medicine Bow orogenic belt based on published data and results presented in this study. Area is not conserved between parts A–D, and upper-crustal features are exaggerated for clarity. (A) Pre–1780 Ma passive margin along the southern edge of the Wyoming Province (after Karlstrom and Houston, 1984). (B) The ca. 1780 Ma tectonic event of Jones et al. (2010) telescoped the passive-margin sequence and juxtaposed the Wyoming and Colorado Provinces. (C) Circa 1763 Ma extension was largely confined to the Green Mountain terrane (after Jones et al., 2010). (D) Final accretion of the Green Mountain terrane at ca. 1750 Ma drove orogenesis and formation of the Cheyenne belt shear zones as a sinistral transpressional stretching fault system.

on the total amount of strike-slip motion. The eastern Bear Lake subterrane may have formed from a reactivated normal fault block from the extended continental margin, whereas the Barber Lake terrane may have formed from a thrust slice between the Green Mountain terrane and the Snowy Pass Supergroup (cf. Figs. 14B and 14D). However, these possibilities are largely unconstrained.

(5) Continued crustal shortening and increased exhumation rates caused a late-phase shift to southeast-side-up motion along much of the Cheyenne belt. This deformation largely overprinted fabrics related to the main-phase sinistral oblique transpressional deformation.

Two observations support the interpretation that differential penetrative horizontal shortening resulted in significant crustal thickness variations across the Cheyenne belt. First, deformation fabrics south of the Cheyenne belt throughout the Medicine Bow Mountains are characterized by subvertical foliations, but evidence for Paleoproterozoic penetrative horizontal shortening north of the suture zone is largely restricted to the upper Libby Creek Group (Houston et al., 1968; Karlstrom and Houston, 1984). Second, seismic data indicate that the crust south of the Cheyenne belt is currently ~10 km thicker than the crust north of the belt (Smithson and Boyd, 1998; Crosswhite and Humphreys, 2003; Morozova et al., 2005).

The principle of isostasy dictates that most crustal thickening takes place by displacing the mantle rather than building orogenic welts. Therefore, crustal thickening results in net downward displacement of material at most crustal levels (cf. Fig. 14D). Downward displacement during crustal thickening can account for northwest-side-up motion in the northern mylonite zone at the Bear Lake locality. Additionally, the flattening of this downward flow at deep crustal levels can explain the apparent interwedging nature of the Cheyenne belt recognized in seismic-reflection profiles (Morozova et al., 2005). It is unclear whether the inferred late-stage change in kinematic geometry from sinistral, northwest-side-up, oblique-slip motion to predominately southeast-side-up, dip-slip motion represents a shift in relative plate motions. A simpler explanation may be that the component of sinistral strike-slip motion was partitioned elsewhere in the orogen as deformation progressed. One possible candidate for this deformation is the Moose Mountain shear zone, located ~100 km south of the Cheyenne belt in the Colorado Province (Selverstone et al., 2000). This shear zone separates two distinctly different Paleoproterozoic terranes and records ca. 1720 Ma sinistral strike-slip deformation (Selverstone et al., 2000).

Comparisons with Existing Models and Additional Tests

Our model for the evolution of the Cheyenne belt is similar to existing models in that it relies heavily on the existing plate-tectonic framework and invokes rotation and transposition of initially shallowly dipping structures during subsequent penetrative horizontal shortening (cf. Hills and Houston, 1979; Karlstrom and Houston, 1984; Duebendorfer and Houston, 1986, 1987; Jones et al., 2010). Our model differs from previously published models in that: (1) it invokes two distinct phases of crustal contraction north of the Cheyenne belt that were separated temporally by extension in the Green Mountain terrane (cf. Jones et al., 2010); (2) the main phase of deformation occurred while the shear zones were subvertical (cf. Hills and Houston, 1979; Karlstrom and Houston, 1984; Duebendorfer and Houston, 1986, 1987); and (3) this main phase of deformation accommodated sinistral strike-slip motion and differential crustal thickening across the belt (cf. Hills and Houston, 1979; Karlstrom and Houston, 1984; Duebendorfer and Houston, 1986, 1987).

Several additional tests will help to further constrain models of the Cheyenne belt. Careful direct dating of the different kinematic domains at the Bear Lake and Middle Fork localities may help constrain the timing of deformation and test our interpretation of two distinct kinematic phases during ca. 1750 Ma crustal shortening. Additional direct dating of deformation north and south of the Cheyenne belt will help to test our interpretation of two distinct phases of crustal contraction north of the belt. Finally, detailed structural analyses and thermobarometry of rocks in the Medicine Bow Mountains south of the Cheyenne belt will help to constrain the overall architecture of the Medicine Bow orogeny.

Our field observations and kinematic analyses can also be explained by variable transposition of earlier tectonic fabrics during pervasive simple shearing of all of the rocks in the belt (cf. Williams and Jiang, 2005). In such an interpretation, some of the different kinematic domains may represent inherited fabrics that were not completely overprinted during foliation transposition. This interpretation is supported by the regional parallelism of foliations and tectonic contacts and by the observation that the compositional layering in the mylonitic banded gneiss and biotite gneiss was indeed transposed from an earlier gneissic structure. However, the kinematic indicators used in our analyses formed during pervasive dynamic recrystallization and grain-size reduction. Such fabrics typically do not survive subsequent metamorphism and deformation because the large grain-boundary and internal-strain potential energies cause them to rapidly recrystallize. Additionally, the biotite and banded gneiss mylonites record the same combined sense of motion (sinistral/northwest-side-up oblique slip) as mylonites of the French Slate. The French Slate does not have a pre-Cheyenne belt tectonic fabric. Therefore, we find it unlikely that a significant number of kinematic indicators in our dataset were inherited from an earlier deformation phase. Additionally, many of the rocks that contain evidence for sinistral strike-slip motion in the Middle Fork and Bear Mountain localities are younger than 1780 Ma, and they also do not exhibit any evidence for a pre-Cheyenne belt fabric.

Regional Correlations

Our model, like many of the existing models for the Cheyenne belt (e.g., Hills and Houston, 1979; Karlstrom and Houston, 1984; Duebendorfer and Houston, 1987), is largely based on geologic data from the northeast-striking segment of the belt exposed in the Medicine Bow Mountains (Fig. 1). West of the Medicine Bow Mountains, the Cheyenne belt is roughly east-northeast or east striking (Fig. 1, inset) (Sears et al., 1982). It is quite possible that convergence between the Wyoming Province and the Green Mountain terrane was roughly north-south directed in present-day coordinates. This convergence would lead to sinistral transpression along the northeast-striking segment of the Cheyenne belt and near-orthogonal convergence west of the Medicine Bow Mountains. Unfortunately, the original geometry of the Cheyenne belt is completely obscured by later deformation and magmatism west and east of the Medicine Bow Mountains (Hills and Houston, 1979; Houston and Graff, 1995; Frost et al., 1999; Duebendorfer et al., 2006), and direct regional correlations are impossible. However, several researchers have recognized high-temperature, penetrative crustal shortening and northeast-striking, reverse-sinistral, oblique-slip shear zones north of the inferred trace of the Cheyenne belt in the Laramie Mountains (e.g., Chamberlain et al., 1993; Bauer et al., 1996; Allard, 2003; Resor and Snoke, 2005).

ACKNOWLEDGMENTS

Field work was funded by two Colby College Natural Science Division grants to Sullivan. Scanning electron microscope and electron backscatter diffraction work was funded by a Mellon Foundation Collaborative Faculty Enhancement grant to Sullivan and Beane and by National Science Foundation grant MRI-0320871 to Beane. Sullivan was assisted in the field by M. Jadkowski and W. Fereday. D. Jones graciously guided us to the Bear Mountain locality outcrop, and Jones and A.W. Snoke provided insightful discussions about the Precambrian geology of southeastern Wyoming. R.A. Gastaldo helped us craft our writing for a general audience. The orientation data

in Figure 3 were plotted using the program Stereonet created by R. Allmendinger. Reviews by two anonymous reviewers, L.J.H. D'el-Rey Silva, A.W. Snoke, and M. Williams helped improve the final version of this manuscript, but any remaining errors of omission or interpretation are our own.

REFERENCES CITED

Allard, S.T., 2003, Geologic Evolution of Archean and Paleoproterozoic Rocks in the Northern Palmer Canyon Block, Central Laramie Mountains, Albany County, Wyoming [Ph.D. dissertation]: Laramie, Wyoming, University of Wyoming, 316 p.

Ball, T.T., and Farmer, G.L., 1991, Identification of 2.0 to 2.4 Ga Nd model age crustal material in the Cheyenne belt, southeastern Wyoming: Implications for Proterozoic accretionary tectonics at the southern margin of the Wyoming craton: Geology, v. 19, p. 360–363, doi:10.1130/0091-7613(1991)019<0360:IOTGNM>2.3.CO;2.

Bauer, R.L., Chamberlain, K.R., Snoke, A.W., Frost, B.R., Resor, P.G., and Gresham, A.D., 1996, Ductile deformation of mid-crustal Archean rocks in the foreland of Early Proterozoic orogenies, central Laramie Mountains, Wyoming, *in* Thompson, R.A., Hudson, M.R., and Pillmore, C.L., eds., Geologic Excursions in the Rocky Mountains and Beyond: Field Trip Guide Book for the 1996 Annual Meeting of the Geological Society of America: Colorado Geological Survey (CD-ROM).

Berthé, D., Choukroune, P., and Gapais, D., 1979, Orthogneiss mylonite and non-coaxial deformation of granites: The example of the South Armorican shear zone: Journal of Structural Geology, v. 1, p. 31–42, doi: 10.1016/0191-8141(79)90019-1.

Bickford, M.E., and Hill, B.M., 2007, Does the arc accretion model adequately explain the Paleoproterozoic evolution of southern Laurentia? An expanded interpretation: Geology, v. 35, p. 167–170, doi:10.1130/G23174A.1.

Bowring, S.A., and Karlstrom, K.E., 1990, Growth, stabilization, and reactivation of Proterozoic lithosphere in the southwestern United States: Geology, v. 18, p. 1203–1206, doi:10.1130/0091-7613(1990)018<1203:GSAROP>2.3.CO;2.

Chamberlain, K.R., 1998, Medicine Bow orogeny: Timing of deformation and model of crustal structure produced during continent-arc collision, ca. 1.78 Ga, southeastern Wyoming: Rocky Mountain Geology, v. 33, p. 259–277.

Chamberlain, K.R., Patel, S.C., Frost, B.R., and Snyder, G.L., 1993, Thick-skinned deformation of the Archean Wyoming Province during Proterozoic arc-continental collision: Geology, v. 21, p. 995–998, doi:10.1130/0091-7613(1993)021<0995:TSDOTA>2.3.CO;2.

Condie, K.C., and Shadel, C.A., 1984, An Early Proterozoic volcanic arc succession in southeastern Wyoming: Canadian Journal of Earth Sciences, v. 21, p. 415–427, doi:10.1139/e84-045.

Crosswhite, J.A., and Humphreys, E.D., 2003, Imaging the mountainless root of the 1.8 Ga Cheyenne belt suture and clues to its tectonic stability: Geology, v. 31, p. 669–672, doi:10.1130/G19552.1.

Czeck, D.M., and Hudleston, P.J., 2003, Testing models for obliquely plunging lineations in transpression: A natural example and theoretical discussion: Journal of Structural Geology, v. 25, p. 959–982, doi:10.1016/S0191-8141(02)00079-2.

Dewey, J.F., Holdsworth, R.E., and Strachan, R.A., 1998, Transpression and transtension zones, *in* Holdsworth, R.E., Strachan, R.A., and Dewey, J.F., eds., Continental Transpressional and Transtensional Tectonics: Geological Society of London Special Publication 135, p. 1–14.

Duebendorfer, E.M., 1986, Structure, Metamorphism, and Kinematic History of the Cheyenne Belt, Medicine Bow Mountains, Southeastern Wyoming [Ph.D. dissertation]: Laramie, Wyoming, University of Wyoming, 323 p.

Duebendorfer, E.M., 1988, Evidence for an inverted metamorphic gradient associated with a Precambrian suture, southern Wyoming: Journal of Metamorphic Geology, v. 6, p. 41–63, doi:10.1111/j.1525-1314.1988.tb00407.x.

Duebendorfer, E.M., 1990, Geologic Map of the Cheyenne Belt, Medicine Bow Mountains, Wyoming: Geological Survey of Wyoming Map OF-90-S, scale 1:24,000 and 1:48,000, 2 sheets.

Duebendorfer, E.M., and Houston, R.S., 1986, Kinematic history of the Cheyenne belt, Medicine Bow Mountains, southeastern Wyoming: Geology, v. 14, p. 171–174, doi:10.1130/0091-7613(1986)14<171:KHOTCB>2.0.CO;2.

Duebendorfer, E.M., and Houston, R.S., 1987, Proterozoic accretionary tectonics at the southern margin of the Archean Wyoming craton: Geological Society of America Bulletin, v. 98, p. 554–568, doi:10.1130/0016-7606(1987)98<554:PATATS>2.0.CO;2.

Duebendorfer, E.M., Chamberlain, K.R., and Heizler, M.T., 2006, Filling the North American Proterozoic tectonic gap: 1.60–1.59-Ga deformation and orogenesis in southern Wyoming, USA: The Journal of Geology, v. 114, p. 19–42, doi:10.1086/498098.

Dutton, B.J., 1997, Finite strains in transpression zones with no boundary slip: Journal of Structural Geology, v. 19, p. 1189–1200, doi:10.1016/S0191-8141(97)00043-6.

Etchecopar, A., and Malavieille, J., 1987, Computer models of pressure shadows: A method for strain measurement and shear sense determination: Journal of Structural Geology, v. 9, p. 667–677, doi:10.1016/0191-8141(87)90151-9.

Fossen, H., and Tikoff, B., 1993, The deformation matrix for simultaneous simple shearing, pure shearing and volume change, and its application to transpression-transtension tectonics: Journal of Structural Geology, v. 15, p. 413–422, doi:10.1016/0191-8141(93)90137-Y.

Frost, C.D., Frost, B.R., Chamberlain, K.R., and Edwards, B.R., 1999, Petrogenesis of the 1.43 Ga Sherman batholith, SE Wyoming, USA: A reduced, rapakivi-type anorogenic granite: Journal of Petrology, v. 40, p. 1771–1802, doi:10.1093/petroj/40.12.1771.

Fynn, G.W., and Powell, W.J.A., 1979, The Cutting and Polishing of Electro-Optic Materials: London, Adam Hilger, 216 p.

Giorgis, S., and Tikoff, B., 2004, Constraints on kinematics and strain from feldspar porphyroclast populations, *in* Alsop, I., and Holdsworth, R., eds., Transport and Flow Processes in Shear Zones: Geological Society of London Special Publication 224, p. 265–285.

Greene, D.C., and Schweickert, R.A., 1995, The Gem Lake shear zone: Cretaceous dextral transpression in the Northern Ritter Range pendant, eastern Sierra Nevada, California: Tectonics, v. 14, p. 945–961, doi:10.1029/95TC01509.

Hemmingway, B.R., Robie, R.A., Evans, H.T., and Kerrick, D.M., 1991, Heat capacities and entropies of sillimanite, fibrolite, andalusite, kyanite, and quartz and the Al_2SiO_5 phase diagram: The American Mineralogist, v. 76, p. 1597–1613.

Hills, F.A., and Houston, R.S., 1979, Early Proterozoic tectonics of the central Rocky Mountains: North America: Contributions to Geology, University of Wyoming, v. 17, p. 89–109.

Hills, F.A., Gast, P.W., Houston, R.S., and Swainback, I.G., 1968, Precambrian geochronology of the Medicine Bow Mountains, southeastern Wyoming: Geological Society of America Bulletin, v. 79, p. 1757–1784.

Hirth, G., and Tullis, J., 1992, Dislocation creep regimes in quartz aggregates: Journal of Structural Geology, v. 14, p. 145–159, doi:10.1016/0191-8141(92)90053-Y.

Hodges, K.V., and Spear, F.S., 1982, Geothermometry, geobarometry, and the Al_2SiO_5 triple point at Mt. Moosilauke, New Hampshire: The American Mineralogist, v. 67, p. 1118–1134.

Hoffman, P.F., 1988, United plates of America, the birth of a craton: Early Proterozoic assembly and growth of Laurentia: Annual Review of Earth and Planetary Sciences, v. 16, p. 543–603, doi:10.1146/annurev.ea.16.050188.002551.

Houston, R.S., 1968, A Regional Study of Rocks of Precambrian Age in that Part of the Medicine Bow Mountains Lying in Southeastern Wyoming—With a Chapter on the Relationship between Precambrian and Laramide Structure: Geological Survey of Wyoming Memoir 1, 167 p.

Houston, R.S., 1993, Late Archean and Early Proterozoic geology of southeastern Wyoming, *in* Snoke, A.W., Steidtmann, J.R., and Roberts, S.M., eds., Geology of Wyoming: Geological Society of Wyoming Memoir 5, p. 79–116.

Houston, R.S., and Graff, P.J., 1995, Geologic Map of Precambrian Rocks of the Sierra Madre, Carbon County, Wyoming, and Jackson and Routt Counties, Colorado: U.S. Geological Survey Miscellaneous Investigation Map I-2452, scale 1:50,000, 1 sheet.

Houston, R.S., and Karlstrom, K.E., 1992, Geologic Map of Precambrian Metasedimentary Rocks of the Medicine Bow Mountains, Albany and Carbon Counties, Wyoming: U.S. Geological Survey Miscellaneous Investigations Series Map I-2280, scale 1:50,000, 1 sheet.

Houston, R.S., Duebendorfer, E.M., Karlstrom, K.M., and Premo, W.R., 1989, A review of the geology and structure of the Cheyenne belt and Proterozoic rocks of southern Wyoming, *in* Grambling, J.A., and Tewksbury, B.J., eds., Proterozoic Geology of the Southern Rocky Mountains: Geological Society of America Special Paper 235, p. 1–12.

Irwin, W.P., 1972, Terranes of the Western Paleozoic and Triassic Belt in the Southern Klamath Mountains, California: U.S. Geological Survey Professional Paper 800–C, p. C103–C111.

Jiang, D., and Williams, P.F., 1998, High-strain zones: A unified model: Journal of Structural Geology, v. 20, p. 1105–1120, doi:10.1016/S0191-8141(98)00025-X.

Jones, D.S., 2011, Was the Cheyenne belt once a transform margin?: Implications of detrital zircon ages from the Green Mountain arc and Barber Lake block, southern Wyoming: Geological Society of America Abstracts with Programs, v. 43, no. 4, p. 71.

Jones, D.S., Snoke, A.W., Premo, W.R., and Chamberlain, K.R., 2010, New models for Paleoproterozoic orogenesis in the Cheyenne belt region: Evidence from the geology and U-Pb geochronology of the Big Creek Gneiss, southeastern Wyoming: Geological Society of America Bulletin, v. 122, p. 1877–1898, doi:10.1130/B30164.1.

Jones, D.S., Barnes, C.G., Premo, W.R., and Snoke, A.W., 2011, The geochemistry and petrogenesis of the Paleoproterozoic Green Mountain arc: A composite(?), bimodal, oceanic, fringing arc: Precambrian Research, v. 185, p. 231–249, doi:10.1016/j.precamres.2011.01.011.

Jones, R.R., Holdsworth, R.E., Clegg, P., McCaffrey, K., and Tavarnelli, E., 2004, Inclined transpression: Journal of Structural Geology, v. 26, p. 1531–1548, doi:10.1016/j.jsg.2004.01.004.

Karlstrom, K.A., and Houston, R.A., 1984, The Cheyenne belt: Analysis of a Proterozoic suture in southern Wyoming: Precambrian Research, v. 25, p. 415–446, doi:10.1016/0301-9268(84)90012-3.

Karlstrom, K.A., Flurkey, A.J., and Houston, R.S., 1983, Stratigraphy and depositional setting of Proterozoic metasedimentary rocks in southeastern Wyoming: Record of an Early Proterozoic Atlantic-type cratonic margin: Geological Society of America Bulletin, v. 94, p. 1257–1294, doi:10.1130/0016-7606(1983)94<1257:SADSOT>2.0.CO;2.

Krieger-Lassen, N.C., 1996, The relative precision of crystal orientations measured from electron backscattering patterns: Journal of Microscopy, v. 181, p. 72–81, doi:10.1046/j.1365-2818.1996.95376.x.

Kuiper, Y.D., Lin, S., and Jiang, D., 2011, Deformation partitioning in transpressional shear zones with an along-strike stretch component: An example from the Superior boundary zone, Manitoba, Canada: Journal of Structural Geology, v. 33, p. 192–202, doi:10.1016/j.jsg.2010.07.003.

Law, R.D., 1986, Relationships between strain and quartz crystallographic fabrics in the Roche Maurice quartzites of Plougastel, western Brittany: Journal of Structural Geology, v. 8, p. 493–515, doi:10.1016/0191-8141(86)90001-5.

Law, R.D., Schmid, S.M., and Wheeler, J., 1990, Simple shear deformation and quartz crystallographic fabrics: A possible natural example from the Torridon area of NW Scotland: Journal of Structural Geology, v. 12, p. 29–45, doi:10.1016/0191-8141(90)90046-2.

Lin, S., and Williams, P.F., 1992, The origin of ridge-in-groove slickenside striae and associated steps in an S-C mylonite: Journal of Structural Geology, v. 14, p. 315–321, doi:10.1016/0191-8141(92)90089-F.

Lister, G.S., and Hobbs, B.E., 1980, The simulation of fabric development during plastic deformation and its application to quartzite: The influence of deformation history: Journal of Structural Geology, v. 2, p. 355–370, doi:10.1016/0191-8141(80)90023-1.

Lister, G.S., and Snoke, A.W., 1984, S-C mylonites: Journal of Structural Geology, v. 6, p. 617–638, doi:10.1016/0191-8141(84)90001-4.

MacCready, T., 1996, Misalignment of quartz *c*-axis fabrics and lineations due to oblique final strain increments in the Ruby Mountains core complex, Nevada: Journal of Structural Geology, v. 18, p. 765–776, doi:10.1016/S0191-8141(96)80010-1.

Means, W.D., 1989, Stretching faults: Geology, v. 17, p. 893–896, doi:10.1130/0091-7613(1989)017<0893:SF>2.3.CO;2.

Morozova, E.A., Wan, X., Chamberlain, K.R., Smithson, S.B., Johnson, R., and Karlstrom, K.E., 2005, Inter-wedging nature of the Cheyenne belt: Archean-Proterozoic suture defined by seismic reflection data, *in* Karlstrom, K.E., and Keller, G.R., eds., The Rocky Mountain Region—An Evolving Lithosphere: Tectonics, Geochemistry, and Geophysics: American Geophysical Union Geophysical Monograph 154, p. 217–226.

Passchier, C.W., and Simpson, C., 1986, Porphyroclast systems as kinematic indicators: Journal of Structural Geology, v. 8, p. 831–843, doi:10.1016/0191-8141(86)90029-5.

Platt, J.P., and Vissers, R.L.M., 1980, Extensional structures in anisotropic rocks: Journal of Structural Geology, v. 2, p. 397–410, doi:10.1016/0191-8141(80)90002-4.

Premo, W.R., and Loucks, R.R., 2000, Age and Rb-Sr-Nd isotopic systematics of plutonic rocks from the Green Mountain magmatic arc, southeastern Wyoming: Isotopic characterization of a Paleoproterozoic island arc system: Rocky Mountain Geology, v. 35, p. 51–70, doi:10.2113/35.1.51.

Premo, W.R., and Van Schmus, W.R., 1989, Zircon geochronology of Precambrian rocks in southeastern Wyoming and northern Colorado, *in* Grambling, J.A., and Tewksbury, B.J., eds., Proterozoic Geology of the Southern Rocky Mountains: Geological Society of America Special Paper 235, p. 13–32.

Prior, D.J., Mariani, E., and Wheeler, J., 2009, EBSD in the Earth Sciences: Applications, common practice and challenges, *in* Schwartz, A.D., Kumar, M., Adams, B.L., and Field, D.P., eds., Electron Backscatter Diffraction in Materials Science (2nd ed.): New York, Springer, p. 345–360.

Reed, J.C., Jr., Bickford, M.E., Premo, W.R., Aleinikoff, J.N., and Pallister, J.S., 1987, Evolution of the Early Proterozoic Colorado Province: Constraints from U-Pb geochronology: Geology, v. 15, p. 861–865, doi:10.1130/0091-7613(1987)15<861:EOTEPC>2.0.CO;2.

Resor, P.G., and Snoke, A.W., 2005, Laramie Peak shear system, central Laramie Mountains, Wyoming USA: Regeneration of the Archean Wyoming Province during Paleoproterozoic accretion, *in* Bruhn, D., and Burlini, L., eds., High-Strain Zones: Structure and Physical Properties: Geological Society of London Special Publication 245, p. 81–107.

Sanderson, D.J., and Marchini, W.R.D., 1984, Transpression: Journal of Structural Geology, v. 6, p. 449–458, doi:10.1016/0191-8141(84)90058-0.

Sands, D.E., 1969, Introduction to Crystallography: New York, W.A. Benjamin, 165 p.

Schmid, S.M., and Casey, M., 1986, Complete fabric analysis of some commonly observed quartz *c*-axis patterns, *in* Hobbs, B.E., and Heard, C., eds., Mineral and Rock Deformation: Laboratory Studies—The Paterson Volume: American Geophysical Union Geophysical Monograph 36, p. 263–286.

Schmidt, N.H., and Olesen, N.O., 1989, Computer-aided determination of crystal lattice orientation from electron channeling patterns in the SEM: Canadian Mineralogist, v. 27, p. 15–22.

Sears, J.W., Graff, P.J., and Holden, G.S., 1982, Tectonic evolution of Lower Proterozoic rocks, Uinta Mountains, Utah and Colorado: Geological Society of America Bulletin, v. 93, p. 990–997, doi:10.1130/0016-7606(1982)93<990:TEOLPR>2.0.CO;2.

Selverstone, J., Hodgins, M., Aleinikoff, J.N., and Fanning, C.M., 2000, Middle Proterozoic reactivation of an Early Proterozoic transcurrent boundary in the northern Colorado Front Range: Implications for ca. 1.7 and 1.4 Ga tectonism: Rocky Mountain Geology, v. 35, p. 139–162.

Simpson, C., and Schmid, S.M., 1983, An evaluation of criteria to deduce the sense of movement in sheared rocks: Geological Society of America Bulletin, v. 94, p. 1281–1288, doi:10.1130/0016-7606(1983)94<1281:AEOCTD>2.0.CO;2.

Smithson, S.B., and Boyd, N.K., 1998, Geophysical constraints on the deep structure of the Cheyenne belt, southeastern Wyoming: Rocky Mountain Geology, v. 33, p. 279–292.

Spear, F.S., 1993, Metamorphic Phase Equilibria and Pressure-Temperature-Time Paths: Washington, D.C., Mineralogical Society of America, 799 p.

Spear, F.S., and Cheney, J.T., 1989, A petrogenetic grid for pelitic schists in the system SiO_2-Al_2O_3-FeO-MgO-K_2O-H_2O: Contributions to Mineralogy and Petrology, v. 101, p. 149–164, doi:10.1007/BF00375302.

Stipp, M., Stünitz, H., Heilbronner, R., and Schmid, S.M., 2002a, Dynamic recrystallization of quartz: Correlation between natural and experimental conditions, *in* de Meer, S., Drury, M.R., de Bresser, J.H.P., and Pennock, G.M., eds., Deformation Mechanisms, Rheology and Tectonics: Current Status and Future Perspectives: Geological Society of London Special Publication 200, p. 171–190.

Stipp, M., Stünitz, H., Heilbronner, R., and Schmid, S.M., 2002b, The eastern Tonale fault zone: A 'natural laboratory' for crystal plastic deformation of quartz over a temperature range from 250 to 700 °C: Journal of Structural Geology, v. 24, p. 1861–1884, doi:10.1016/S0191-8141(02)00035-4.

Strickland, D., 2004, Structural and Geochronologic Evidence for the Ca. 1.6 Ga Reactivation of the Cheyenne Belt, Southeastern Wyoming [M.S. thesis]: Laramie, Wyoming, University of Wyoming, 157 p.

Sullivan, W.A., 2012, L tectonites: Journal of Structural Geology, doi:10.1016/j.jsg.2012.01.022 (in press).

Sullivan, W.A., and Beane, R.J., 2010, Asymmetrical quartz crystallographic fabrics produced during constrictional deformation: Journal of Structural Geology, v. 32, p. 1,430–1,443, doi:10.1016/j.jsg.2010.08.001.

Sullivan, W.A., and Law, R.D., 2007, Deformation path partitioning within the transpressional White Mountain shear zone, California and Nevada: Journal of Structural Geology, v. 29, p. 583–599, doi:10.1016/j.jsg.2006.11.001.

Sullivan, W.A., Beane, R.J., Beck, E.N., Fereday, W.H., and Roberts-Pierel, A.M., 2011, Testing the transpression hypothesis in the western part of the Cheyenne belt, Medicine Bow Mountains, southeastern Wyoming: Rocky Mountain Geology, v. 46, p. 111–135, doi:10.2113/gsrocky.46.2.111.

ten Grotenhuis, S.M., Trouw, R.A.J., and Passchier, C.W., 2003, Evolution of mica fish in mylonitic rocks: Tectonophysics, v. 372, p. 1–21, doi:10.1016/S0040-1951(03)00231-2.

Tikoff, B., and Greene, D., 1997, Stretching lineations in transpressional shear zones: An example from the Sierra Nevada Batholith, California: Journal of Structural Geology, v. 19, p. 29–39, doi:10.1016/S0191-8141(96)00056-9.

Tullis, J., and Yund, R.A., 1987, Transition from cataclastic flow to dislocation creep of feldspar; mechanisms and microstructures: Geology, v. 15, p. 606–609, doi:10.1130/0091-7613(1987)15<606:TFCFTD>2.0.CO;2.

Tyson, A.R., Morozova, E.A., Karlstrom, K.E., Chamberlain, K.R., Smithson, S.B., Dueker, K.G., and Foster, C.T., 2002, Proterozoic Farwell Mountain–Lester Mountain suture zone, northern Colorado: Subduction flip and progressive assembly of arcs: Geology, v. 30, p. 943–946, doi:10.1130/0091-7613(2002)030<0943:PFMLMS>2.0.CO;2.

Wallis, S.R., 1992, Vorticity analysis in a metachert from the Sanbagawa belt, SW Japan: Journal of Structural Geology, v. 14, p. 271–280, doi:10.1016/0191-8141(92)90085-B.

Warner, L.A., 1978, The Colorado lineament: A middle Precambrian wrench fault system: Geological Society of America Bulletin, v. 89, p. 161–171, doi:10.1130/0016-7606(1978)89<161:TCLAMP>2.0.CO;2.

Whitmeyer, S.J., and Karlstrom, K.E., 2007, Tectonic model for the Proterozoic growth of North America: Geosphere, v. 3, p. 220–259, doi:10.1130/GES00055.1.

Williams, P.F., and Jiang, D., 2005, An investigation of lower crustal deformation: Evidence for channel flow and its implications for tectonics and structural studies: Journal of Structural Geology, v. 27, p. 1486–1504.

Xypolias, P., 2010, Vorticity analysis in shear zones: A review of methods and applications: Journal of Structural Geology, v. 32, p. 2072–2092, doi:10.1016/j.jsg.2010.08.009.

Science Editor: A. Hope Jahren
Associate Editor: An Yin

Manuscript Received 30 January 2012
Revised Manuscript Received 5 December 2012
Manuscript Accepted 17 January 2013

Printed in the USA